Int. J. Adv. Eng. Pure Sci. 2022, 34(1): 167-189
DOI: 10.7240/jeps.993459

RESEARCH ARTICLE / ARAŞTIRMA MAKALESİ

Projections of Future Change of Climatology and Extreme Weather Events in the Mediterranean Basin, by the HIRHAM5 Regional Climate Model

HIRHAM5 Bölgesel İklim Modeli Kullanılarak Akdeniz Havzası'nın Gelecek Klimatolojisi ve Uç Hava Olaylarındaki Değişikliklerin Projeksiyonları

Tugba OZTURK[1,2]

[1] *Department of Physics, Faculty of Engineering and Natural Sciences, Isik University, 34980, Istanbul, Turkey*
[2] *Center for Climate Change and Policy Studies, Bogazici University, 34342, Istanbul, Turkey*

Abstract
In this study, changes in temperature and precipitation climatology and extreme weather events over the Mediterranean Basin including Turkey were investigated using HIRHAM5 driven by global climate models such as EC-EARTH, HadGEM2-ES, and NorESM1-M for 2011-2100 compared to 1971-2000. RCP4.5 and RCP8.5 scenario outputs of global climate models were used as forcing data. Daily mean temperature and precipitation variables are used to compute extreme indices. Extreme indices were calculated for the period of 2071-2100 compared to the reference period. According to the results, the severity of temperature- and precipitation-based indices will be expected to increase throughout the century with increasing radiative forcing. Minimum of minimum temperatures will increase more pronounced over the northern Mediterranean, which is referred to as climate change hot spots, whereas the increase in a maximum of maximum temperatures is moderate over land areas. A decrease in total wet-day precipitation is expected while the number of dry days is expected to increase. Therefore, the Mediterranean Basin and Turkey will have warmer and drier conditions compared to present climate conditions.
Keywords: Climate change, Extreme weather events, HIRHAM5, Regional climate modeling, The Mediterranean Basin, Turkey.

Öz
Bu çalışmada, 1971–2000 referans dönemine göre 2011-2100 gelecek dönemi için Türkiye'nin de dahil olduğu Akdeniz Havzası üzerinde sıcaklık ve yağış klimatolojilerinde ve aşırı hava olaylarındaki öngörülen değişiklikler, EC-EARTH, HadGEM2-ES ve NorESM1-M olmak üzere üç küresel iklim modeli çıktılarıyla koşulan HIRHAM5 bölgesel iklim modeli benzetimleri kullanılarak değerlendirildi. Küresel iklim modellerinin RCP4.5 ve RCP8.5 senaryo çıktıları kullanıldı. Ekstrem iklim indekslerini hesaplamak için sıcaklık ve yağış değişkenlerinin günlük ortalamaları kullanıldı. Ekstrem iklim indekslerindeki değişim yüzyılın sonu olan 2071-2100 yıllarında 1971-2000 referans dönemine göre hesaplandı. Sonuçlara göre, artan ışınımsal zorlamayla birlikte yüzyıl boyunca sıcaklık ve yağış temelli ekstrem hava olaylarının daha şiddetlenmesi beklenmektedir. Minimum sıcaklıklardaki artış, iklim değişikliğinin en önemli sıcak noktalarından biri olması beklenen Akdeniz Havzası'nın kuzey kesiminde daha belirginken, maksimum sıcaklıklardaki artış ise karalar üzerinde ılımlıdır. Art arda gelen kurak günlerin sayısındaki artışla birlikte toplam yağışlı gün sayılarında azalma beklenmektedir. Bu nedenle, Akdeniz Havzası ve Türkiye üzerindeki iklim koşullarının daha sıcak ve daha kurak olması öngörülmektedir.
Anahtar Kelimeler: Akdeniz Havzası, Aşırı Hava Olayları, Bölgesel İklim Modellemesi, HIRHAM5, İklim Değişikliği, Türkiye.

I. INTRODUCTION

Climate change is a major problem for human beings in this century. Climate change, which has a different impact in different regions of the world, affects many different areas such as human health, agriculture and food supply, freshwater resources, and sea-level rise and it threatens not only human beings but also all living organisms. Additionally, changes in the frequency and intensity of extreme events have been observed. According to the latest report of the Intergovernmental Panel on Climate Change (AR6), it is certain that human influence warms the atmosphere, ocean, and soil. Widespread and rapid changes have occurred in the atmosphere, ocean, cryosphere, and biosphere, and human influence has warmed the climate at an unprecedented rate in at least the last 2,000 years and those changes are unprecedented for centuries and millennia. Each of the last 4 decades since 1850 has been warmer than the decade that preceded it [1].

Results of the climate model projections show that the larger Mediterranean Basin including Turkey has been specified as the climate change hot spot by previous studies [2-7]. According to the model results, warming will

Corresponding Author: Tugba OZTURK, Tel: +90 216 528 7189, e-posta: tugba.ozturk@isikun.edu.tr
Submitted: 09.09.2021, **Revised:** 30.03.2022, **Accepted:** 30.03.2022

be expected to occur over the Mediterranean in this century [8-15]. Interannual temperature variability is also projected to increase in summer [5][8]. Because of an increase in temperature variability with the strong mean warming, the severity of extreme temperatures and the frequency of heatwaves are expected to increase [16]. Model projections agree that in the Mediterranean region, the increase in temperature will be 20% warmer than the global temperature change, and a higher increase is expected to occur in summer. Temperatures in the day are anticipated to increase more than temperatures in the night, indicating an increase in the magnitude of the diurnal range [7].

There will also be an escalation of heat stress in the Mediterranean Basin and the frequency and severity of heatwave days will increase because of projected changes in extreme climate indices for temperature [17-24]. Heat stress is expected to intensify due to right-skewed temperature distribution. According to the projections, larger increases are anticipated in the 95th percentile maximum and minimum temperatures than that of the 75th percentile [18]. The number of occurrences of a heatwave is projected to highly increase in the Mediterranean region changing from about 2 days per summer for the reference period of 1961–1990 to around 6–24 days in 2021–2050 and 27–67 days in 2071–2100 [21]. According to the projections based on CMIP5 multi-model ensembles under RCP8.5, for the Mediterranean region, the highest temperatures are found to increase about 7 ℃ in summer which is among the greatest across all subregions around the world. Tropical nights will also increase by approximately 80 days in the Mediterranean under RCP8.5 [22].

Turkey is also a vulnerable region to climate change since it is one of the Mediterranean countries. Studies on climate change and variability for the Mediterranean Basin by simulating global and regional climate models based on both observation data and various greenhouse gas emission scenarios show that the Mediterranean Basin will be adversely affected by climate change in the future [25-30]. Accordingly, an increase in the number of extremely hot days, the frequency and continuity of heatwaves is expected in the Mediterranean Region [31-37]. There are not many climate model projection studies over Turkey and surrounding regions. Almost all studies were based on results of the regional climate model, RegCM [38-53]. Results based on RegCM driven by different global climate models show warming and drying over Turkey. The temperature will increase from on average 1 ℃ up to 4 ℃ for the period of 2020-2050. According to the results of RegCM driven by HadGEM2-ES under RCP4.5, there will be a 4.0 ℃ increase in temperature for summer in all parts of the region and a 2.0 ℃ increase in temperature for winter. According to the model results except ones driven by HadGEM2-ES under RCP 8.5, precipitation will decrease almost all over the domain which is already dry [54].

Studies of regional climate projections based only on one regional climate model (RegCM) for Turkey and surrounding regions are not adequate. The ensemble approach which is based on the ensemble mean of multi-model results has been an approved technique for several years in the regional modeling community. This leads to international projects involving many model working groups such as PRUDENCE [55-56], ENSEMBLES [57-58] and CORDEX [59-60], providing an opportunity for a better understanding of the change in future climate. The most important reason for the lack of literature in this regard over Turkey is that the regional climate models are not open source and are mostly used by developing centers. HIRHAM5 (a model developed by the Danish Meteorological Institute) was used in this study to obtain 12.5 km simulations [61]. HIRHAM5 has been effectively used as a regional model and applied to the EURO-CORDEX domain including the Mediterranean Basin [62-66]. Simulations are performed by driving the model with EC-EARTH, HadGEM2-ES, NorESM1-M global climate model which has medium, high and low climate sensitivity respectively, under RCP4.5 and RCP8.5. Monthly mean values of temperature and precipitation were used to investigate the change in climatology for 2011-2100 relative to the base period of 1971-2000. Daily minimum, maximum temperature, and precipitation fields were also used to calculate climate indices defined by ETCCDI. Results of HIRHAM5 were also compared with the results of a different model, RegCM [67-68].

II. MATERIALS AND METHOD

In this study, HIRHAM5 was used to project temperature and precipitation climatology over the Mediterranean and Turkey. The HIRHAM is a regional atmospheric climate model based on the HIRLAM [69] and ECHAM models [70], combining the dynamics of the former model with the physical parameterization schemes of the latter. The HIRLAM model – High-Resolution Limited Area Model - is a numerical short-range weather forecasting system (http://hirlam.org) and has been used for routine weather forecasting at various meteorological institutes, i.e. DMI (Denmark), FMI (Finland), IMS (Iceland), KNMI (The Netherlands), met.no (Norway), INM (Spain), and SMHI (Sweden). Results of the model were compared with ERA-interim [71] reanalysis datasets and CRU observational datasets to test its performance [72]. EC-EARTH, HadGEM2-ES, and NorESM1-M global climate models were used as forcing data for future simulations under two RCPs [73-75]. In this study, climate variables for the Mediterranean region and Turkey were simulated via HIRHAM5 under the two different RCPs [75].

RCP4.5, which is a medium-low emission scenario, stabilizes after 2100 at 4.5 W/m^2 without overshoot pathway, while RCP8.5 is the highest of the four reaches at 8.5 W/m^2 in 2100 on a rising trajectory.

The spatial changes in lowest of minimum temperatures (TNn) and highest of maximum temperatures (TXx), the temporal evolution of cold days, cold nights, warm days, and warm nights, and spatial patterns of change in total wet day precipitation and consecutive dry days (CDD) were computed for all datasets and scenario outputs [76-78]. The percentile indices are presented as the percentage of days that exceed the thresholds calculated as percentiles of the 1971-2000 base period. Cold nights, cold days and warm nights, and warm days, which are represented as the percentage of days where TN or TX is less than the 10th or more than the 90th percentile, respectively were considered. In the warm spell duration index (WSDI), the number of days of a year when the daily maximum temperature is more than the 90th percentile for at least six consecutive days were counted. CDD is described by the duration of the longest period of dry days occurred consecutively in a year. Extreme weather indices were calculated for the future period of 2071-2100 compared to the period of 1971-2000.

Table 1. Extreme Climate Indices recommended by ETCCDI.

Label	Index Name	Definition	Unit
TNn	Min TN	Annual minimum of minimum temperature	°C
TXx	Max TX	Annual maximum of maximum temperature	°C
TN10p	Cold Nights	The percentage of days in a year is determined where TN < 10th percentile of minimum temperature	%
TX10p	Cold Days	The percentage of days in a year is determined where TX < 10th percentile of maximum temperature.	%
TN90p	Warm Nights	The percentage of days in a year is determined where TN > 90th percentile of minimum temperature.	%
TX90p	Warm Days	The percentage of days in a year is determined where TX > 90th percentile of maximum temperature.	%
WSDI	Warm Spell Duration	Annual count of days with at least 6 consecutive days when TX > 90th percentile of maximum temperature.	days
PRCPTOT	Total wet-day precipitation	Annual total precipitation in wet days.	mm
CDD	Consecutive Dry Days	The largest number of consecutive days where PR<1 mm.	days

III. RESULTS AND DISCUSSIONS

3.1. Model Performance for Temperature

RCM's performance in simulating present climate conditions was investigated by comparing model results with ERA-interim and CRU for 1971-2000. Results of ERA-Interim are given for 1980-2000 due to the availability of data. Outputs of HIRHAM5, driven by EC-EARTH, HadGEM2-ES, and NorESM1-M are represented in Figure 1-3 together with ERA-interim and CRU respectively. The climatology of model results was calculated for a period of 1971–2000. The results of the model show a much more detailed temperature distribution due to higher resolution (0.11°-12.5 km) compared to ERA-interim (0.75°) and CRU (0.5°) dataset. Comparisons with the observational dataset (CRU) were also given as statistics including bias, Root Mean Square Error (RMSE), and correlation coefficient for mean temperature, maximum and minimum temperature, and precipitation weighted over the domain for each season (Table 2-5). Regional climate model, HIRHAM forced by all three global climate models simulates the spatial and temporal (seasonal) distribution of temperature over the domain. All three model outputs show similar temperature distribution throughout the region except HadGEM2-ES shows warmer temperatures over the Mediterranean Sea and North Africa could be due to high equilibrium climate sensitivity of global climate model HadGEM2-ES. Results of each model produce colder temperatures compared to reanalysis and observational dataset around high topographical regions of the domain like the Alpine region and southeastern Turkey. We also observed this cold bias in outputs of RegCM. This might be because of error in measurements at the stations which were generally built-in valleys of mountains of the region [53]. Excluding the mountainous parts of the domain, HIRHAM5 gives similar results with reanalysis data and observation.

Spatial statistics for seasonal mean temperature were given in Table 1. Results of the ERA-interim dataset and the HIRHAM5 model were compared with the CRU observational datasets. The performance of the reanalysis dataset is better compared to the regional model as expected. A cold bias is seen in the results of EC-EARTH driven HIRHAM5 for every season whereas warm bias is seen in HadGEM2-ES and NorESM1-M driven HIRHAM5 except for summer in NorESM1-M driven HIRHAM5. Even though the results of HIRHAM5 driven by different GCMs are quite similar in magnitude, HadGEM2-ES driven HIRHAM5 model results show better performance compared to other models except for winter if we look at the RMSE values. Winter has larger RMSE values than the other seasons likely due to cold bias around the mountainous region. It is also shown that model results are highly correlated with the observational dataset. Maximum and minimum temperature results of HIRHAM5 driven by three GCMs were also given in Table 3 and Table 4, respectively. Each model result has cold biases for every season regardless of driven GCM for maximum temperature. This could be indicating that future changes in maximum temperature are underestimated by model results. RMSEs are higher than that of mean temperature which is anticipated since the magnitude of maximum temperature is larger than mean temperature. Summer values of RMSE are larger than other seasons in which stronger magnitudes are observed. On the other hand, minimum temperatures are overestimated by the model (Table 4). EC-EARTH driven HIRHAM5 has the highest performance out of the three models according to RMSE values. Both maximum and minimum temperature results are found to be highly correlated with the observational values.

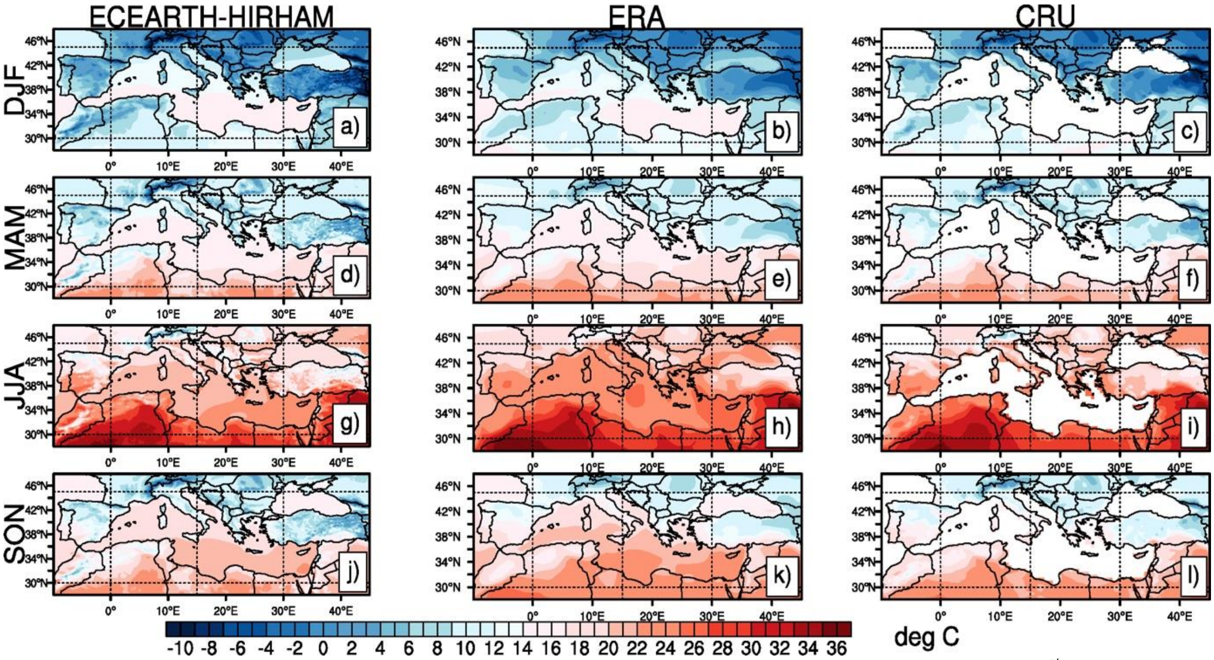

Figure 1. Average temperatures (°C) by HIRHAM5 with EC-EARTH dataset for 1971–2000 (1st column), by ERA-Interim dataset for 1980–2000 (2nd column) and CRU observational temperature dataset for 1971–2000 (3rd column) for winter (a-c), spring (d-f), summer (g-i), autumn (j-l).

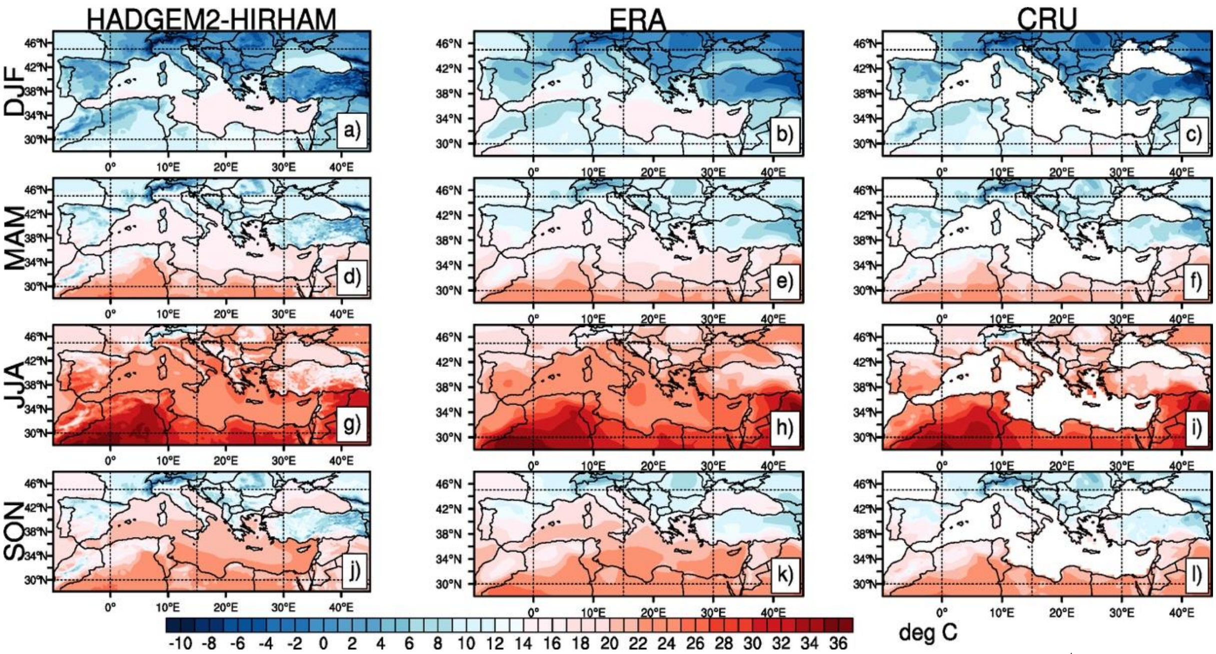

Figure 2. Average temperatures (°C) by HIRHAM5 with HadGEM2-ES dataset for 1971–2000 (1st column), by ERA-Interim dataset for 1980–2000 (2nd column) and CRU observational temperature dataset for 1971–2000 (3rd column) for winter (a-c), spring (d-f), summer (g-i), autumn (j-l).

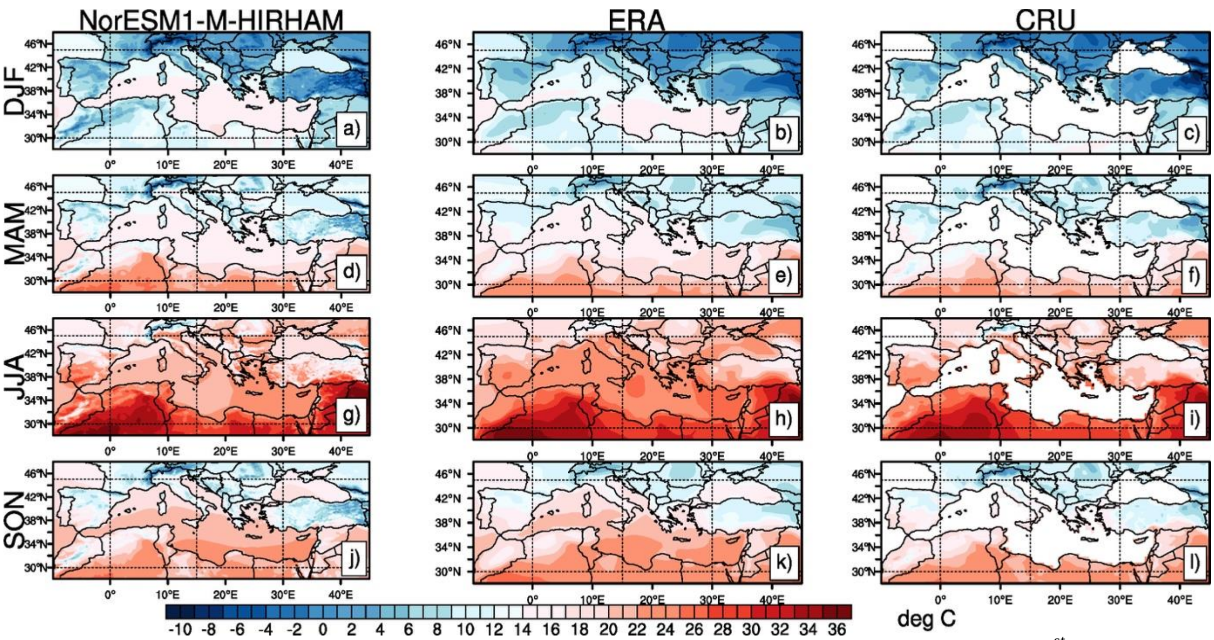

Figure 3. Average temperatures (°C) by HIRHAM5 with NorESM1-M dataset for 1971–2000 (1st column), by ERA-Interim dataset for 1980–2000 (2nd column) and CRU observational temperature dataset for 1971–2000 (3rd column) for winter (a-c), spring (d-f), summer (g-i), autumn (j-l).

Table 2. Statistics for seasonal mean temperature (°C) weighted over the whole domain for the period of 1980-2000 for ERA-interim, and 1971-2000 for HIRHAM5 driven by three global climate models compared to CRU observational dataset.

		ERA-interim	EC-EARTH-HIRHAM	HadGEM2-ES-HIRHAM	NorESM1-M-HIRHAM
DJF	Bias	0.448	-0.321	0.114	1.301
	RMSE	1.244	2.490	2.593	2.882
	Correlation	0.975	0.900	0.881	0.877
MAM	Bias	0.424	-0.624	0.504	0.857
	RMSE	1.042	1.606	1.553	1.777
	Correlation	0.977	0.958	0.955	0.951
JJA	Bias	0.482	-1.700	0.500	-0.660
	RMSE	1.231	2.548	1.809	2.217
	Correlation	0.970	0.944	0.937	0.928
SON	Bias	0.535	-1.160	0.288	0.163
	RMSE	1.068	2.087	1.847	1.835
	Correlation	0.982	0.944	0.937	0.931

Table 3. Statistics for seasonal mean maximum temperature (°C) weighted over the whole domain for the period of 1971-2000 for HIRHAM5 driven by three global climate models compared to CRU observational dataset.

		EC-EARTH-HIRHAM	HadGEM2-ES-HIRHAM	NorESM1-M-HIRHAM
DJF	Bias	-1.776	-1.370	-0.329
	RMSE	2.922	2.880	2.642
	Correlation	0.921	0.907	0.901
MAM	Bias	-2.517	-1.322	-1.079
	RMSE	3.110	2.366	2.388
	Correlation	0.940	0.930	0.920
JJA	Bias	-4.046	-1.896	-3.023
	RMSE	4.848	3.211	4.210
	Correlation	0.901	0.885	0.880
SON	Bias	-3.303	-1.876	-2.043
	RMSE	3.719	2.608	2.829
	Correlation	0.950	0.944	0.935

Table 4. Statistics for seasonal mean minimum temperature (°C) weighted over the whole domain for the period of 1971-2000 for HIRHAM5 driven by three global climate models compared to CRU observational dataset.

		EC-EARTH-HIRHAM	HadGEM2-ES-HIRHAM	NorESM1-M-HIRHAM
DJF	Bias	1.389	1.881	3.148
	RMSE	3.230	3.448	4.197
	Correlation	0.895	0.879	0.874
MAM	Bias	1.393	2.448	2.916
	RMSE	2.468	3.120	3.454
	Correlation	0.937	0.938	0.940
JJA	Bias	0.857	3.053	1.883
	RMSE	2.209	3.569	2.836
	Correlation	0.938	0.935	0.925
SON	Bias	1.282	2.727	2.624
	RMSE	2.583	3.553	3.429
	Correlation	0.924	0.917	0.914

3.2. Model Performance for Precipitation

Average precipitation obtained from the HIRHAM5, driven by EC-EARTH, HadGEM2-ES, and NorESM1-M global dataset, together with ERA-interim and the CRU, is presented in Figure 4-6 respectively. Results give very similar values for each HIRHAM5 output driven by three different global models. We observe slightly more precipitation in the spring season over the Mediterranean Sea for HIRHAM5 driven by EC-EARTH model data than other model results (Figure 4d). Even though the regional climate model reproduces seasonal variability reasonably well, it overestimates precipitation compared to the observation, especially over high plateau regions during the spring, autumn, and winter seasons. Overestimation is independent of the global climate model used to drive the regional climate model, HIRHAM5. This wet bias is also observed in outputs of regional climate model RegCM. It might be because of the bias in the observational dataset as we observed it in temperature outputs as well. However, model outputs agree with reanalysis and observations for summer over Turkey where precipitation amounts have already low values.

Model performance for precipitation was also investigated by looking at spatial statistics over the whole domain given by Table 5. Results were compared with the CRU observational dataset for mean precipitation as well. Negative bias is seen in the ERA-interim results for every season. Model results differ in direction of bias except for negative bias in summer. There is a positive bias for winter in all outputs of HIRHAM5 indicating that it overestimates the precipitation. Bias and RMSE values are smaller for summer since this season is drier compared to other seasons in the region. Winter has higher values of RMSE even if the bias is small possibly because of an overestimation of precipitation values. EC-EARTH driven HIRHAM5 has the lowest RMSE for winter and autumn when the region takes more precipitation compared to other seasons. Even though it is less than temperature, precipitation values are also correlated with the observation.

3.3. Changes in Temperature

Projections of temperature obtained from HIRHAM5 forced by EC-EARTH, HadGEM2-ES, and NorESM1-M based on the RCP4.5 scenario are presented in Figure 7, Figure 9, and Figure 11. Outputs based on RCP8.5 scenarios are also presented in Figure 8, Figure 10, and Figure 12. First, general warming is projected over all parts of the domain throughout the century. Projected warming is increasing and becoming stronger with time and strongest warming is expected in the end-century period. The outputs of all three global model datasets show similar changes with each other. However, the HadGEM2-ES global model has more severe results than EC-EARTH and NorESM1-M especially under RCP8.5 for 2071–2100 very likely due to high climate sensitivity (Figure 12). According to RCP8.5 model scenario results of EC-EARTH and NorESM1-M, the highest warming of 5 °C is found to be in southeast Europe, Turkey, Morocco, Algeria, and the Iberian Peninsula, in summer (Figure 12-g, i) for end century period. HadGEM2-ES model gives more than 6 °C increase over all parts of the domain for summer (Figure 12-h). More warming in Central Europe and North Africa will be observed in winter (Figure 12-a, b). Temperatures will be expected to increase from 3.5 up to 5 °C for spring and autumn (Figure 12-d,e,f and j,k,l). According to RCP4.5 results, warming will be expected to be between 1.5 °C and 5 °C for the period of 2071-2100 (Figure 11). The maximum temperature increase is projected in summer mainly over the regions including Morocco, Algeria, and the Iberian Peninsula (Figure 11-g,h,i). The warming temperature pattern is similar for both scenarios and all periods with summer being the warmest and winter less warm season. Therefore, it is anticipated that the change in temperature over the region will be towards warmer temperatures as time passes. Moreover, the changes will be more severe for RCP8.5 compared to RCP4.5. The regional climate model results of temperature are generally in line with AR6 [1, 29].

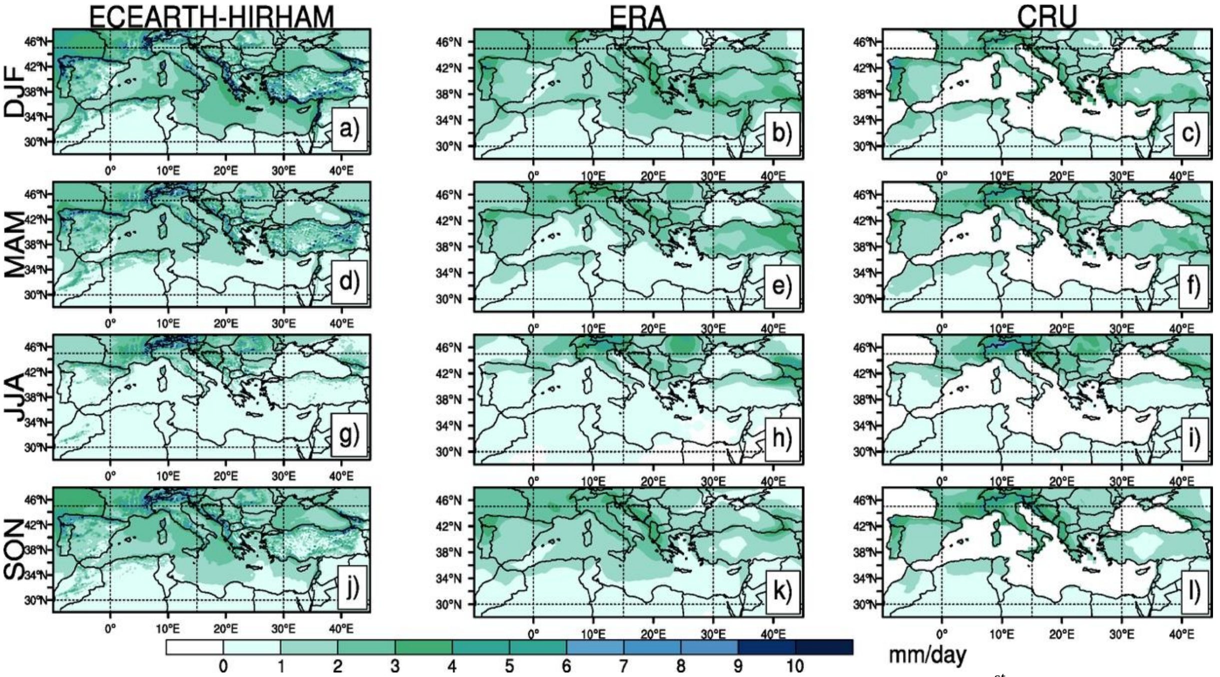

Figure 4. Precipitation (mm/day) by HIRHAM5 with EC-EARTH dataset for 1971–2000 (1st column), by ERA-Interim dataset for 1980–2000 (2nd column) and CRU observational temperature dataset for 1971–2000 (3rd column) for winter (a-c), spring (d-f), summer (g-i), autumn (j-l).

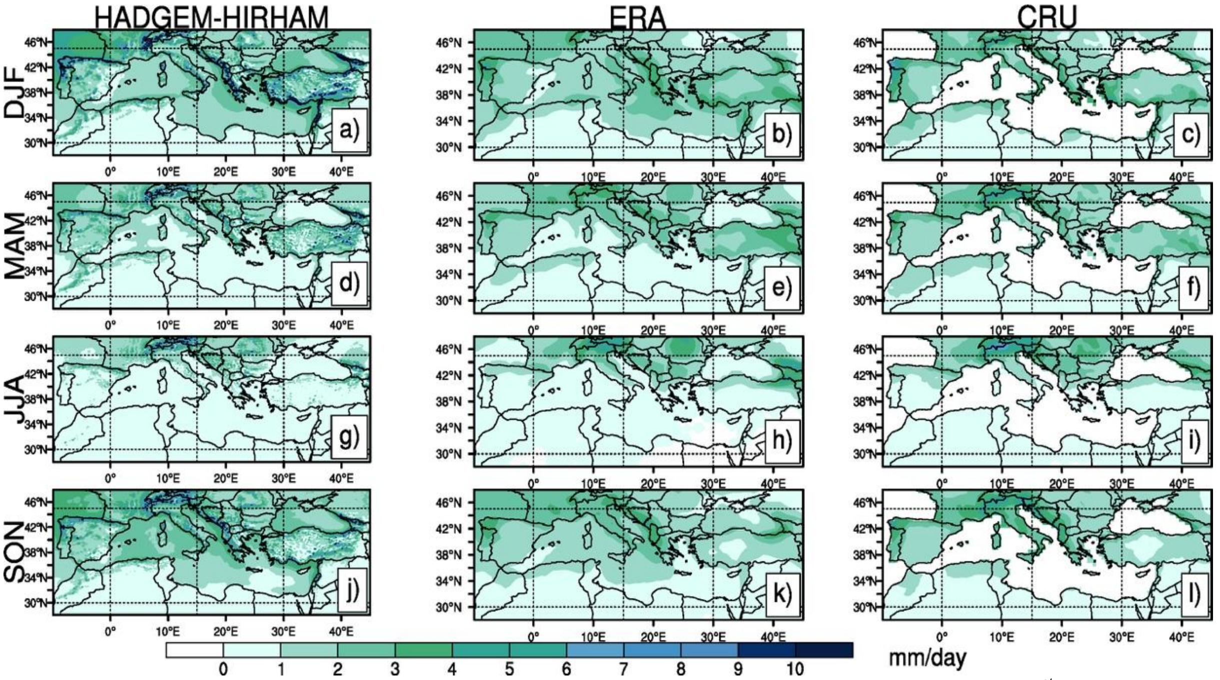

Figure 5. Precipitation (mm/day) by HIRHAM5 with HadGEM2-ES dataset for 1971–2000 (1st column), by ERA-Interim dataset for 1980–2000 (2nd column) and CRU observational temperature dataset for 1971–2000 (3rd column) for winter (a-c), spring (d-f), summer (g-i), autumn (j-l).

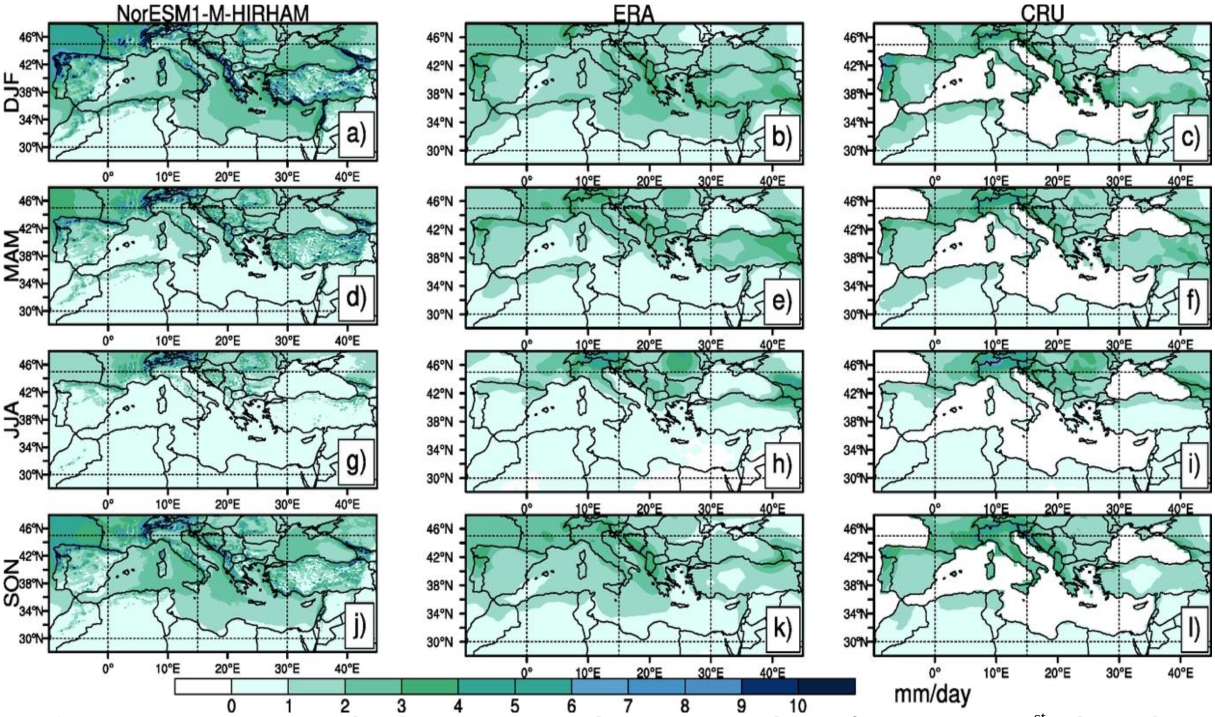

Figure 6. Precipitation (mm/day) by HIRHAM5 with NorESM1-M dataset for 1971–2000 (1st column), by ERA-Interim dataset for 1980–2000 (2nd column) and CRU observational temperature dataset for 1971–2000 (3rd column) for winter (a-c), spring (d-f), summer (g-i), autumn (j-l).

Table 5. Statistics for seasonal mean precipitation (mm/day) weighted over the whole domain for the period of 1980-2000 for ERA-interim, and 1971-2000 for HIRHAM5 driven by three global climate models compared to CRU observational dataset.

		ERA-interim	EC-EARTH-HIRHAM	HadGEM2-ES-HIRHAM	NorESM1-M-HIRHAM
DJF	Bias RMSE Correlation	-0.362 0.650 0.877	0.368 1.768 0.652	0.380 1.949 0.614	0.583 2.286 0.631
MAM	Bias RMSE Correlation	-0.201 0.451 0.902	0.268 1.334 0.716	-0.093 1.089 0.711	0.089 1.362 0.716
JJA	Bias RMSE Correlation	-0.156 0.423 0.935	-0.015 0.850 0.812	-0.241 0.712 0.812	-0.197 0.809 0.797
SON	Bias RMSE Correlation	-0.314 0.548 0.920	0.171 1.145 0.744	0.267 1.245 0.731	0.206 1.301 0.722

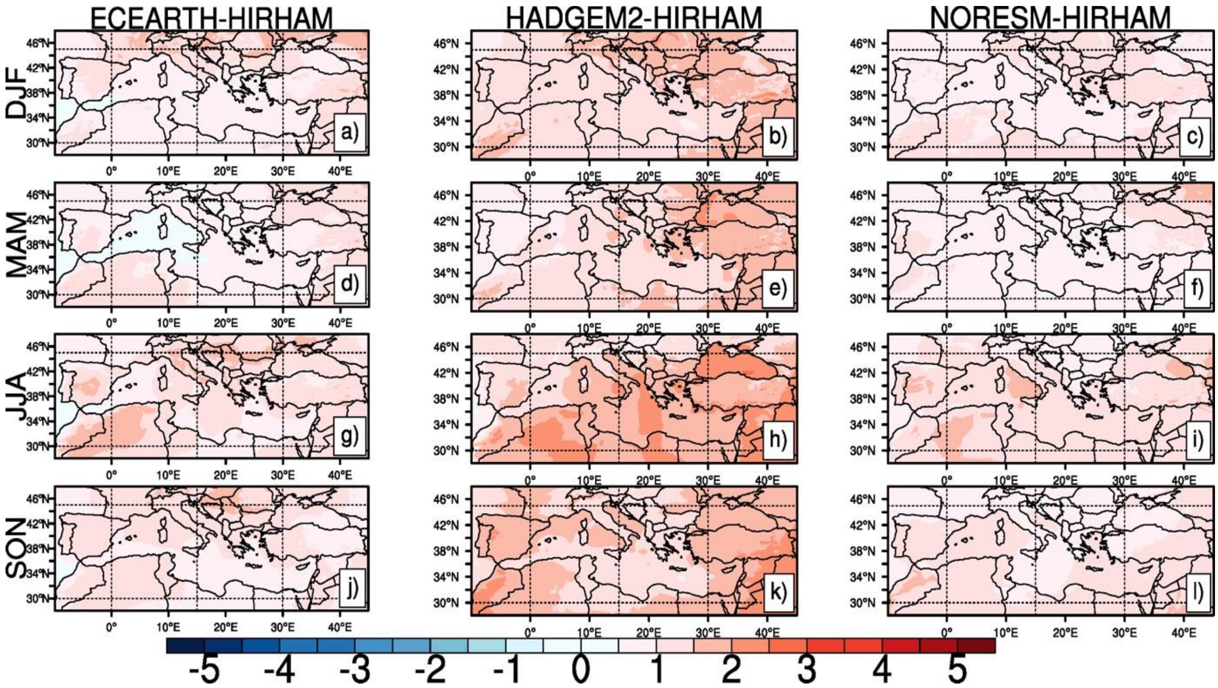

Figure 7. Spatial changes in temperatures (°C) obtained from HIRHAM5, forced by EC-EARTH, HADGEM2-ES, and NORESM1-M with RCP4.5 for 2011–2040, with respect to 1971–2000: (a-c) winter, (d-f) spring, (g-i) summer, (j-l) autumn, respectively.

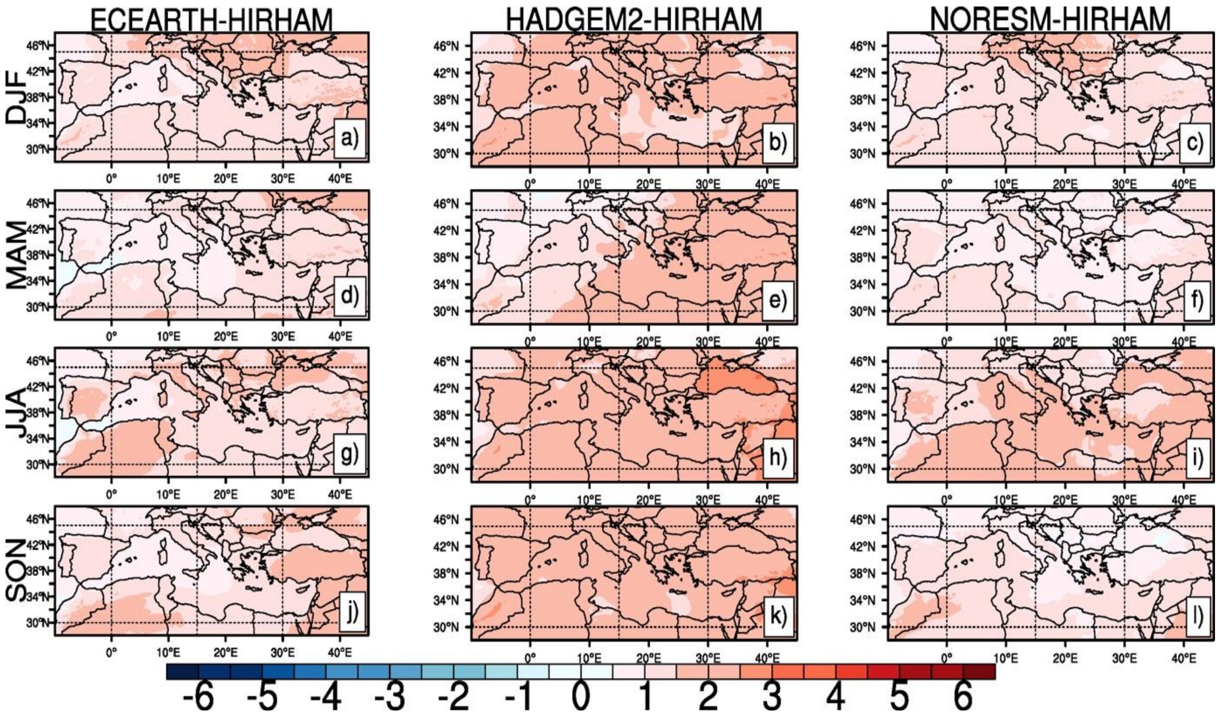

Figure 8. Spatial changes in temperatures (°C) obtained from HIRHAM5, forced by EC-EARTH, HADGEM2-ES, and NORESM1-M with RCP8.5 for 2011–2040, with respect to 1971–2000: (a-c) winter, (d-f) spring, (g-i) summer, (j-l) autumn, respectively.

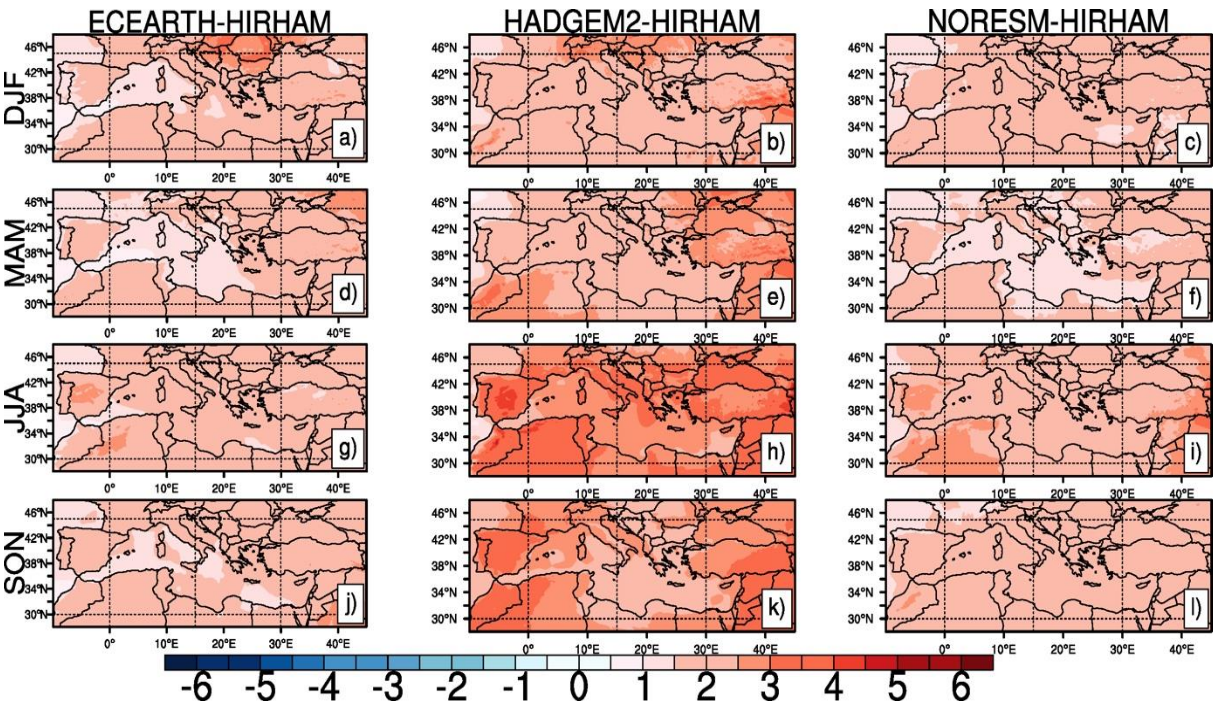

Figure 9. Spatial changes in temperatures (°C) obtained from HIRHAM5, forced by EC-EARTH, HADGEM2-ES, and NORESM1-M with RCP4.5 for 2041–2070, with respect to 1971–2000: (a-c) winter, (d-f) spring, (g-i) summer, (j-l) autumn, respectively.

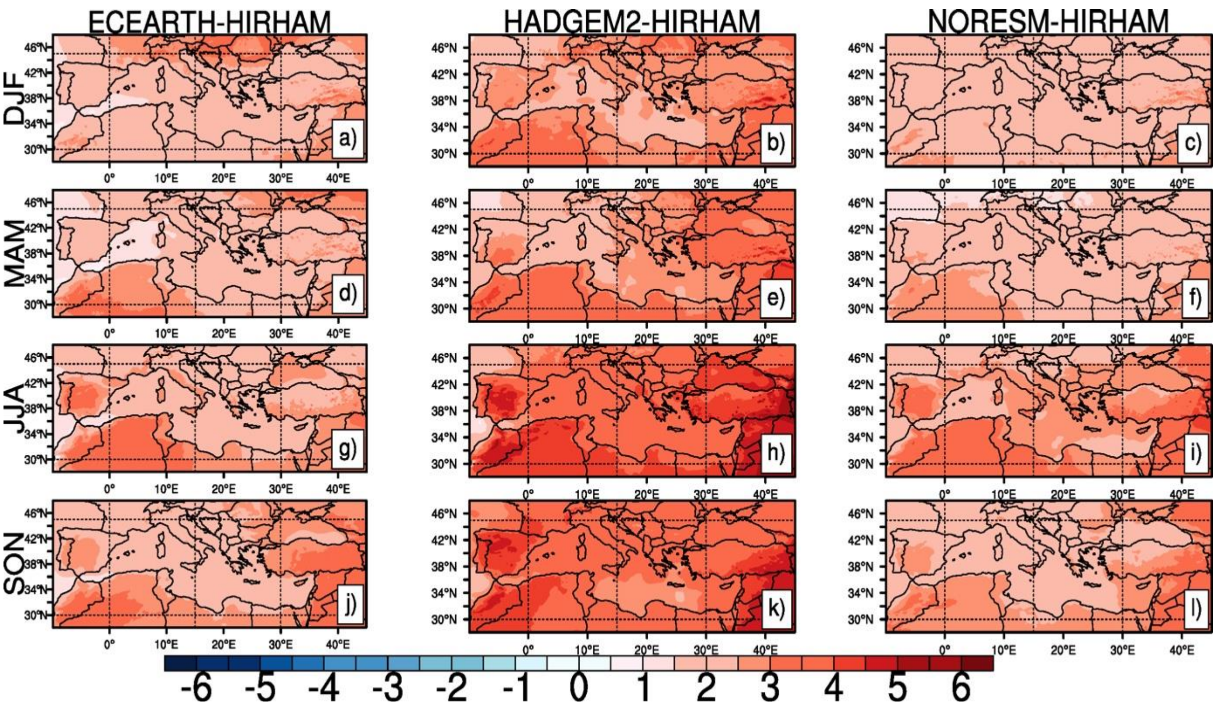

Figure 10. Spatial changes in temperatures (°C) obtained from HIRHAM5, forced by EC-EARTH, HADGEM2-ES, and NORESM1-M with RCP8.5 for 2041–2070, with respect to 1971–2000: (a-c) winter, (d-f) spring, (g-i) summer, (j-l) autumn, respectively.

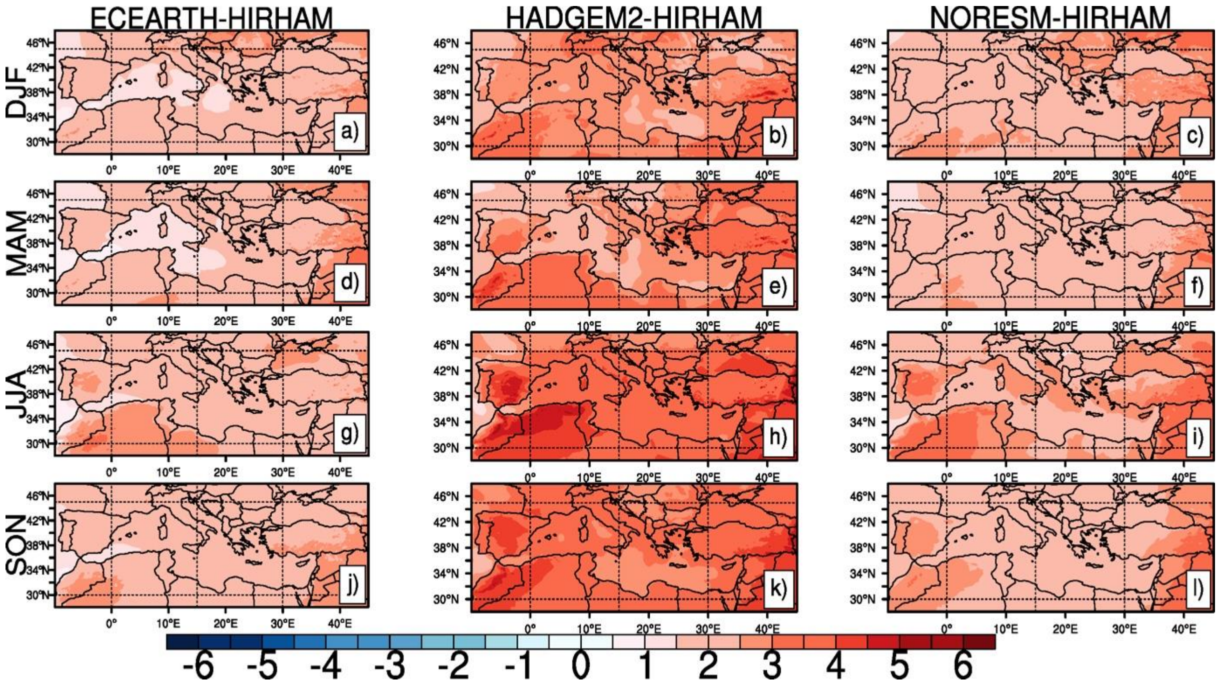

Figure 11. Spatial changes in temperatures (°C) obtained from HIRHAM5, forced by EC-EARTH, HADGEM2-ES, and NORESM1-M with RCP4.5 for 2071–2100, with respect to 1971–2000: (a-c) winter, (d-f) spring, (g-i) summer, (j-l) autumn, respectively.

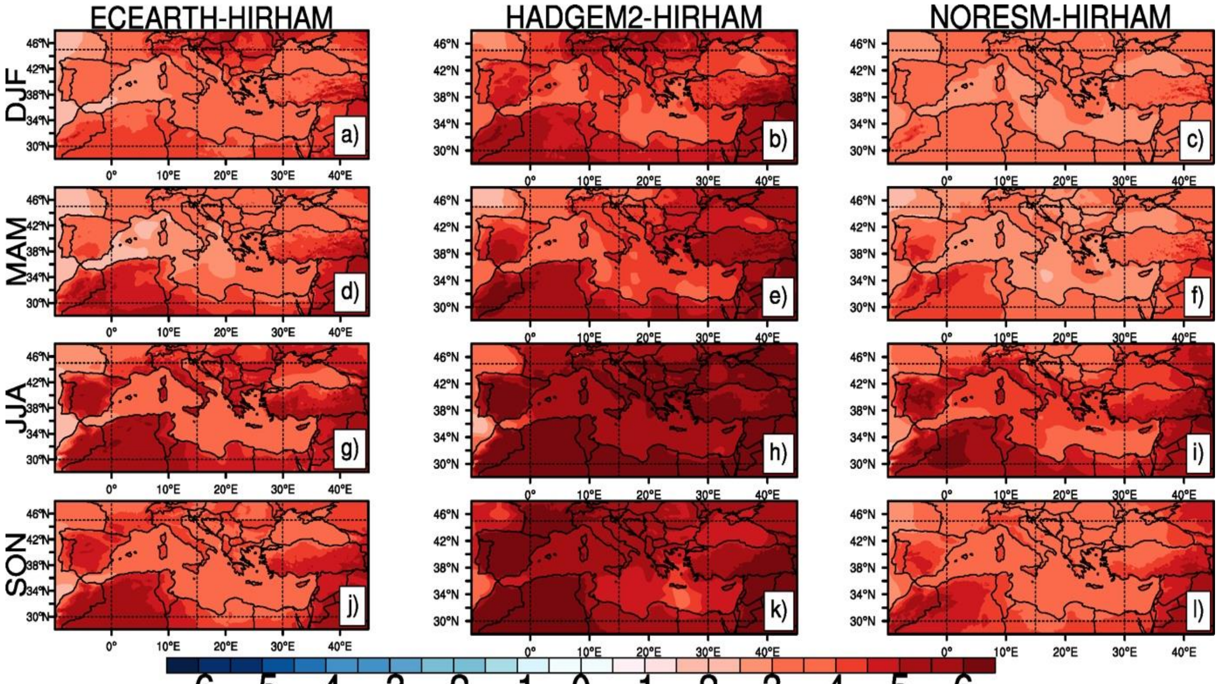

Figure 12. Spatial changes in temperatures (°C) obtained from HIRHAM5, forced by EC-EARTH, HADGEM2-ES, and NORESM1-M with RCP8.5 for 2071–2100, with respect to 1971–2000: (a-c) winter, (d-f) spring, (g-i) summer, (j-l) autumn, respectively.

3.4. Changes in Precipitation

The projection of precipitation changes based on the RCP4.5 is presented in Figures 13, 15, and 17 respectively. Outputs based on RCP8.5 scenarios are also presented in Figure 14, Figure 16, and Figure 18. Even though no pronounced change in the amount of precipitation will be expected over the domain, especially for the near-future period of 2011-2040, the direction of the change is negative except slight increase given by HadGEM2-ES results for the winter over southern Europe and the Iberian Peninsula for both emission scenarios RCP4.5 and RCP8.5 (Figures 13 and 14). The magnitude of decrease in precipitation is projected to be larger for the mid-future period especially over the Iberian Peninsula, and the Alpine region in autumn with a strong decrease simulated by HadGEM2-ES driven HIRHAM (Figure 15 and 16). A decrease in precipitation in the southwest coasts of Turkey will be expected much in the winter for the end-century period (Figure 18-a,b,c). However, models give an increase of precipitation in the north part of Turkey and the Alpine region for winter. Drier conditions will be expected to occur for Turkey for all seasons except winter. Model outputs of RCP8.5 show more intense values than RCP4.5 output. A decrease in precipitation amounts in the Mediterranean Basin will be expected for summer and autumn. This decrease will occur over the north part of the Mediterranean region including the Balkans, France, Italy, and Caucasia. These results are also in line with AR6, stating that South Europe and the Mediterranean Basin will receive a less amount of average precipitation [1, 29].

3.5. Future Changes in Extreme Indices

3.5.1. Absolute temperature indices

Future changes in TXx and TNn for 2071-2100 relative to 1971-2000 for two RCPs are presented in Figures 19 and 20, respectively. The projected changes in TNn and TXx differ from each other spatially. The increase in TNn is higher in northern parts of the region such as central and southern Europe. The highest increase in TNn, up to 12 °C, is projected in RCP8.5 in regions such as the south Balkans and especially the southeastern part of Turkey (Figure 20). Larger changes in TNn in high topographical regions might be associated with snow cover retreatment. Changes in TXx are only moderate over land. The increase in TXx over the Iberian Peninsula is remarkable compared to other land areas, especially for regional climate model outputs driven by the HadGEM2-ES global model. HadGEM2-ES has more severe results than other models for TXx and TNn as well in both RCPs. Nevertheless, TXx warming over the Mediterranean is about 7 °C. Therefore, summer extreme temperatures will be pronouncedly increasing over the region.

3.5.2 Duration temperature index

Projected changes in the warm spell duration over the period of 2071-2100 relative to the base period of 1971-2000 for two RCPs are presented in Figure 21. Consistent with the changes in extreme temperatures, WSDI is expected to increase in both RCPs. Changes in RCP8.5 are again stronger for all simulation results. The greatest increase in WSDI occurs in the Mediterranean Sea and this might be related to WSDI being sensitive to temperature variability which is small in the Mediterranean Sea surface [22]. Results indicate that the duration of warm spell will be more than 100 days longer for the worst-case scenario at the end of the century. This increase will be more in the south part of the Iberian Peninsula and Northern African countries. The southeastern part of Turkey will have around 180 days longer warm spell according to the projections.

3.5.3. Percentile temperature indices

The percentile indices are represented as a percentage of days relative to 1971–2000 (Figure 22). A decrease in the number of cold nights and cold days is projected from the 1970s throughout the century in all model results. The decrease is generally more pronounced in HadGEM2-ES results starting from 2010 (red line). The responses for RCP8.5 are showing a very strong decrease in TN10p and TX10p from about 12% to 0.3%, throughout the century. These results show that almost no cold nights or cold days will occur by the end of the century. Warm nights and days will be expected to increase throughout the 21st century (Figure 22a, b). The increase is again higher in HadGEM2-ES results than the results of other models. The positive change in the number of warm nights and days for RCP8.5 scenarios is from about 10% in 1971–2000 to 84.6%, 76.4%, and 74.9% by 2100 for HadGEM2-ES, EC-EARTH, and NorESM1-M model results, respectively. Results show that more than 75% of the days and nights will be warmer than the 90^{th} percentile of 1971-2000 by the end of the century.

3.5.4. Precipitation indices

Total wet-day precipitation is defined by the amount of precipitation on the day whose precipitation is at least 1 mm. Results are given for the period of 2071-2100 relative to the base period 1971-2000 in % for both scenario outputs in Figure 23. Projected change in CDD is shown in Figure 24. For the end of the century, total wet-day precipitation decreases significantly over southern parts of the region in both RCPs relative to 1971–2000. There is also a slight increase in total wet-day precipitation over southern Europe. Regions in which decreases in total wet-day precipitation are projected will also observe a pronounced increase in CDD. Pronounced increases of CDD occur particularly in northern Africa, the Iberian Peninsula, and the inner regions of Turkey (Figure 24). Slight decreases in CDD are also expected to occur in the Alpine region.

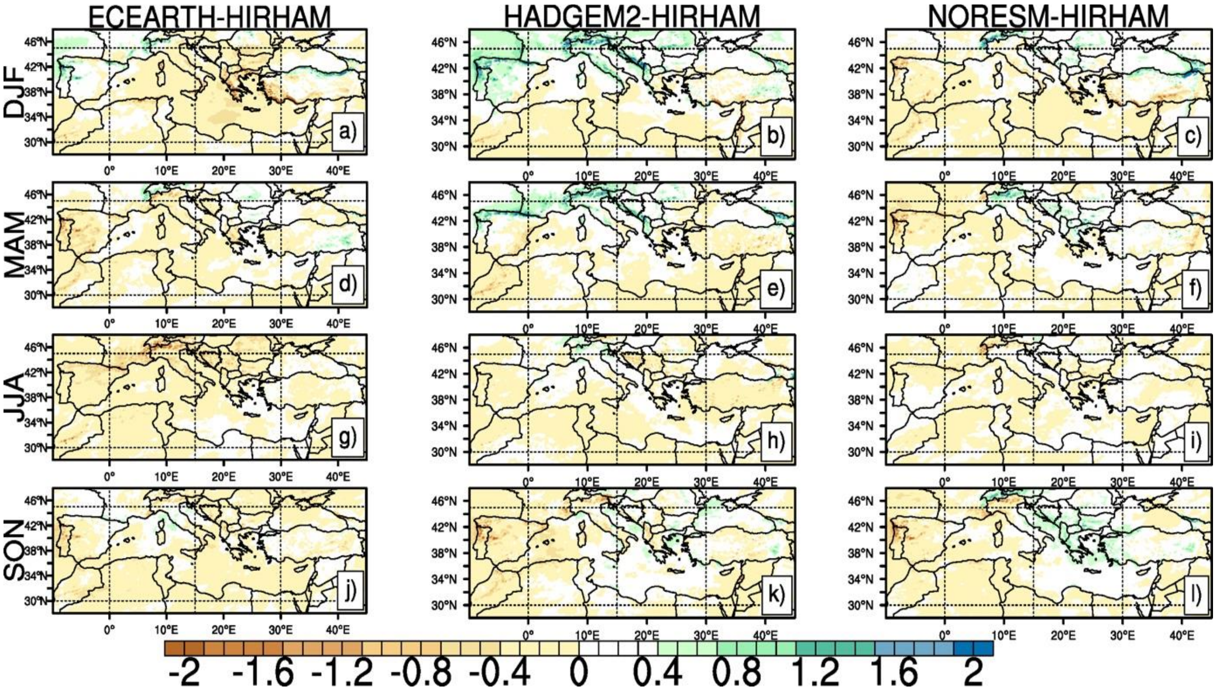

Figure 13. Spatial changes in precipitation (mm/day) obtained from HIRHAM5, forced by EC-EARTH, HADGEM2-ES, and NORESM1-M with RCP4.5 for 2011–2040, with respect to 1971–2000: (a-c) winter, (d-f) spring, (g-i) summer, (j-l) autumn, respectively.

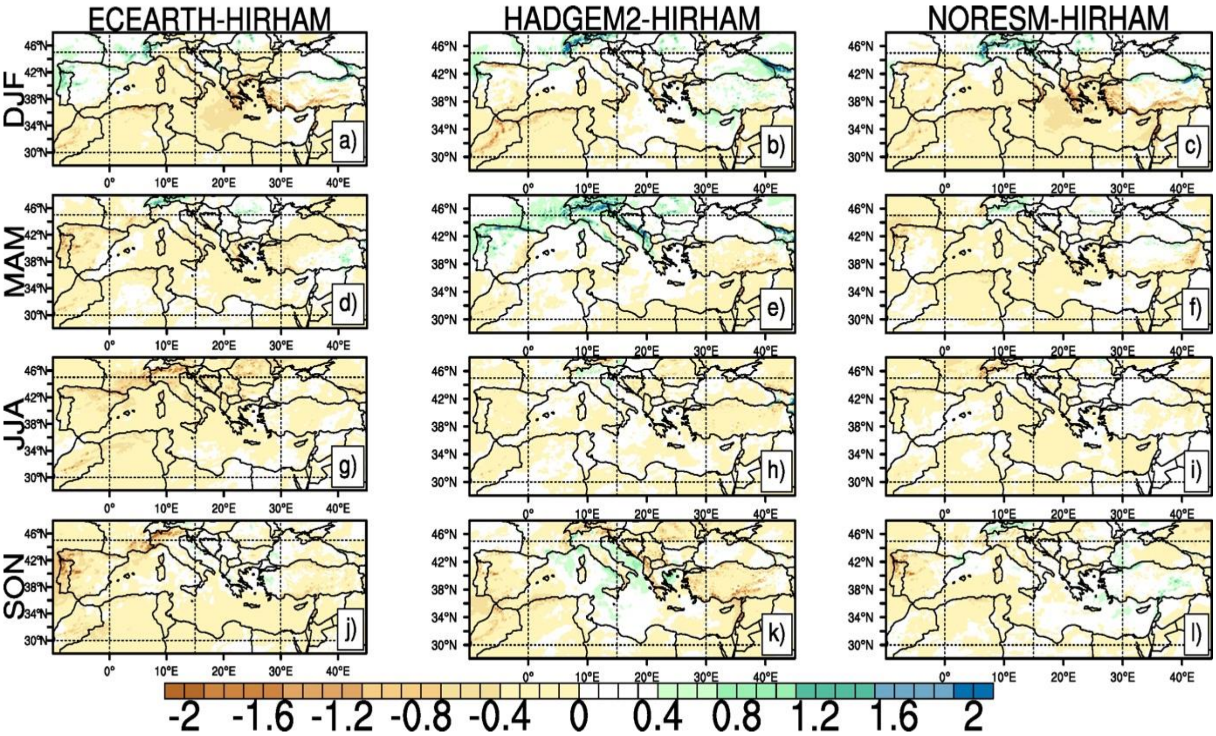

Figure 14. Spatial changes in precipitation (mm/day) obtained from HIRHAM5, forced by EC-EARTH, HADGEM2-ES, and NORESM1-M with RCP8.5 for 2011–2040, with respect to 1971–2000: (a-c) winter, (d-f) spring, (g-i) summer, (j-l) autumn, respectively.

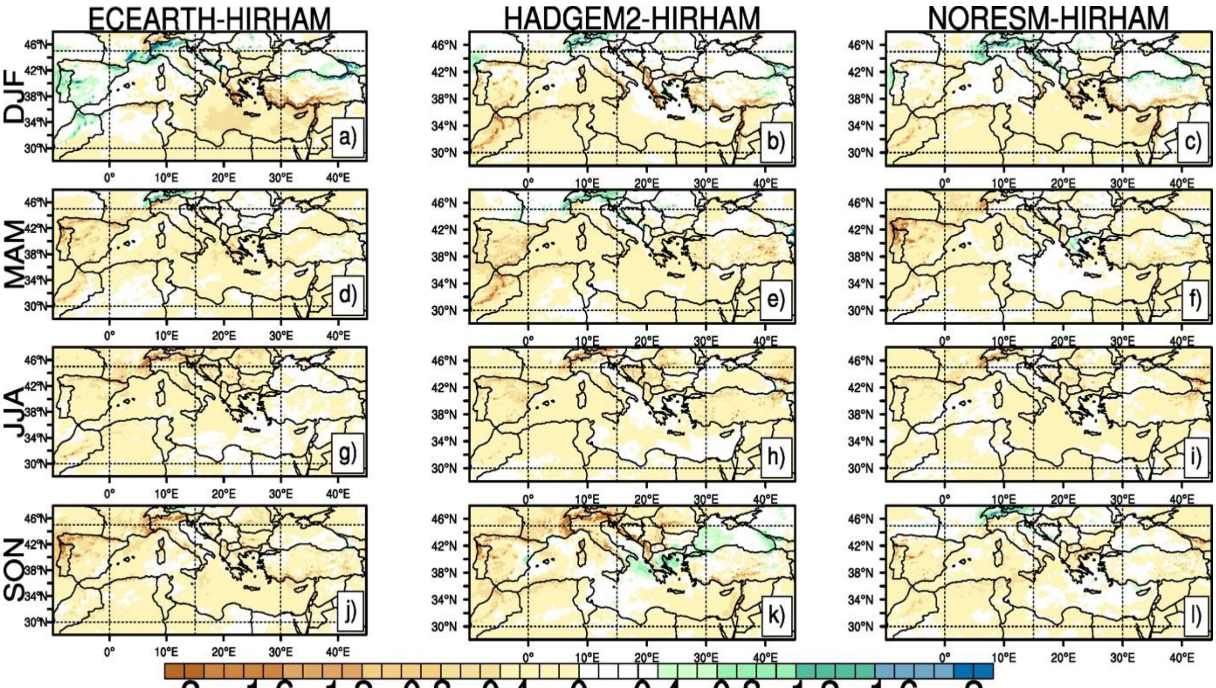

Figure 15. Spatial changes in precipitation (mm/day) obtained from HIRHAM5, forced by EC-EARTH, HADGEM2-ES, and NORESM1-M with RCP4.5 for 2041–2070, with respect to 1971–2000: (a-c) winter, (d-f) spring, (g-i) summer, (j-l) autumn, respectively.

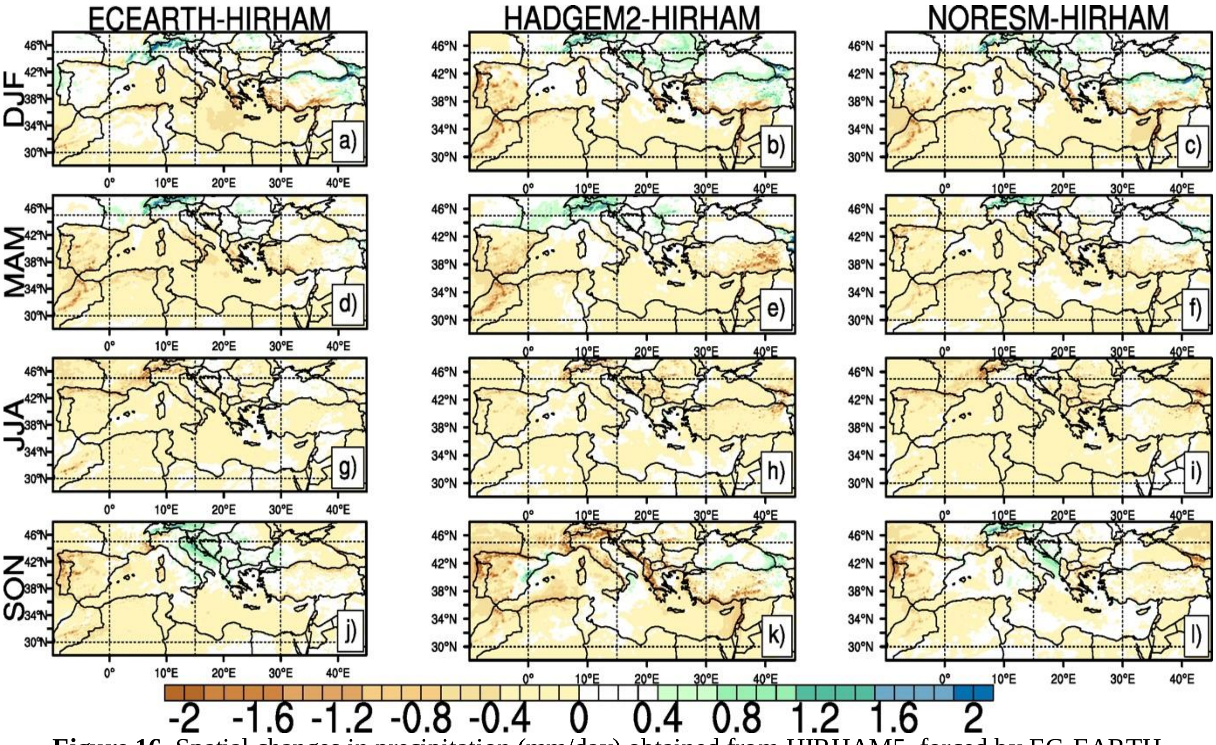

Figure 16. Spatial changes in precipitation (mm/day) obtained from HIRHAM5, forced by EC-EARTH, HADGEM2-ES, and NORESM1-M with RCP8.5 for 2041–2070, with respect to 1971–2000: (a-c) winter, (d-f) spring, (g-i) summer, (j-l) autumn, respectively.

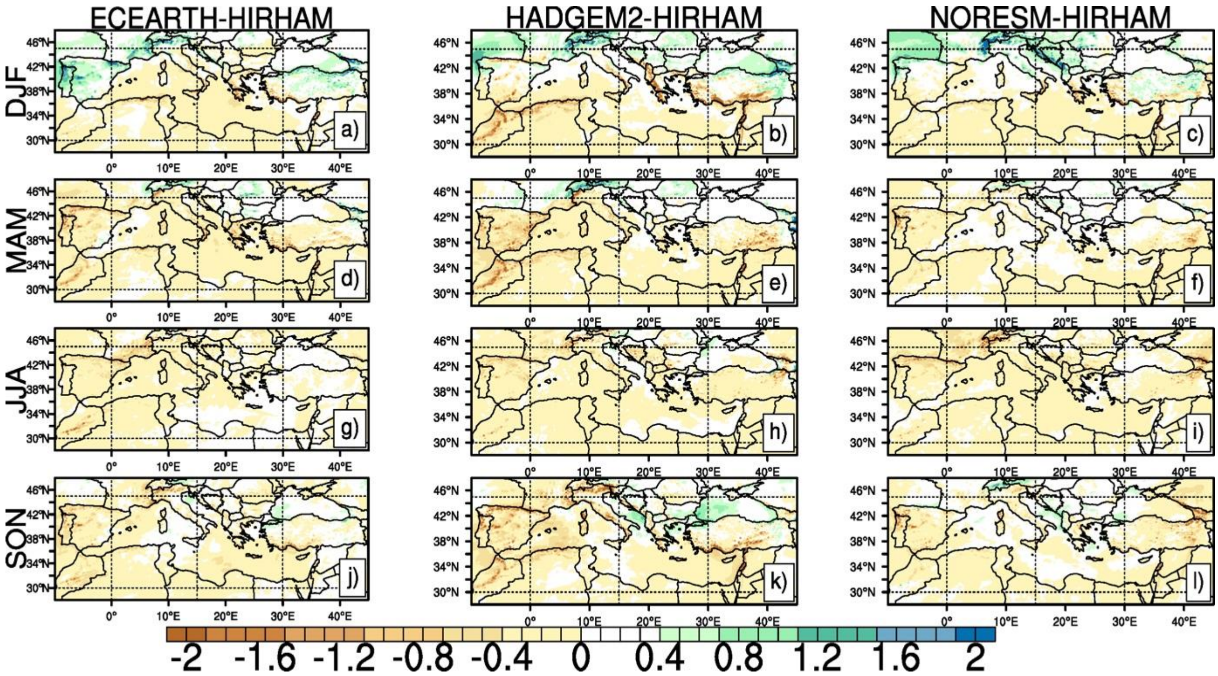

Figure 17. Spatial changes in precipitation (mm/day) obtained from HIRHAM5, forced by EC-EARTH, HADGEM2-ES, and NORESM1-M with RCP4.5 for 2071–2100, with respect to 1971–2000: (a-c) winter, (d-f) spring, (g-i) summer, (j-l) autumn, respectively.

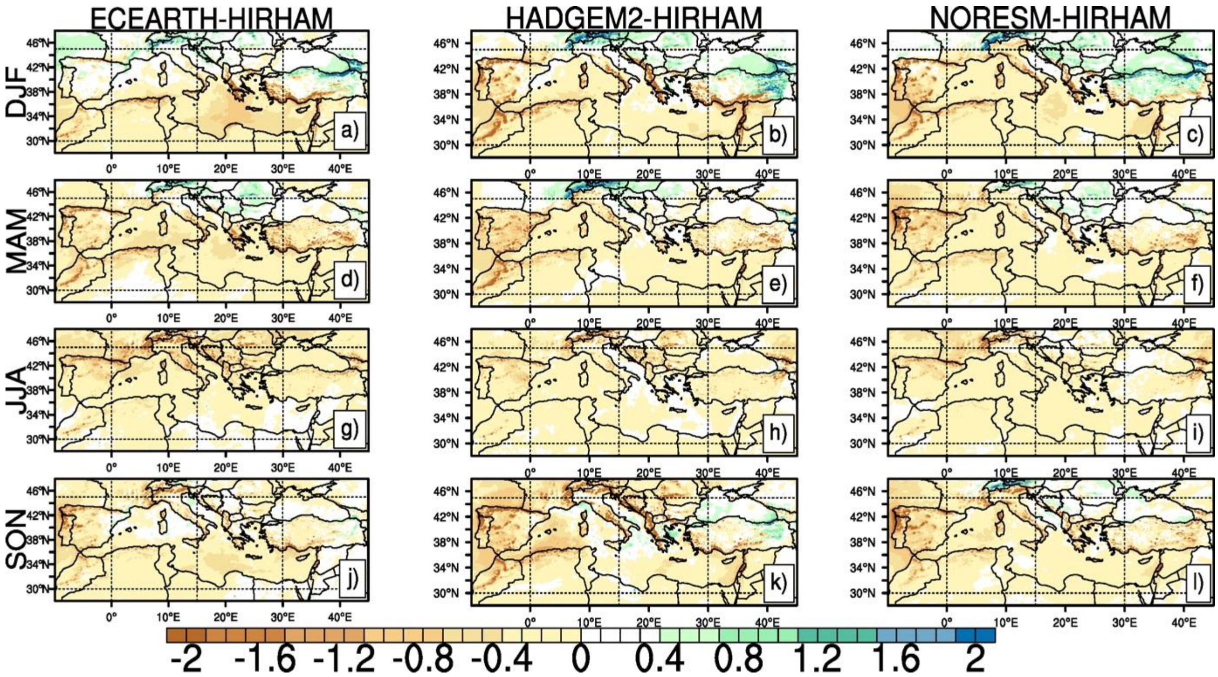

Figure 18. Spatial changes in precipitation (mm/day) obtained from HIRHAM5, forced by EC-EARTH, HADGEM2-ES, and NORESM1-M with RCP8.5 for 2071–2100, with respect to 1971–2000: (a-c) winter, (d-f) spring, (g-i) summer, (j-l) autumn, respectively.

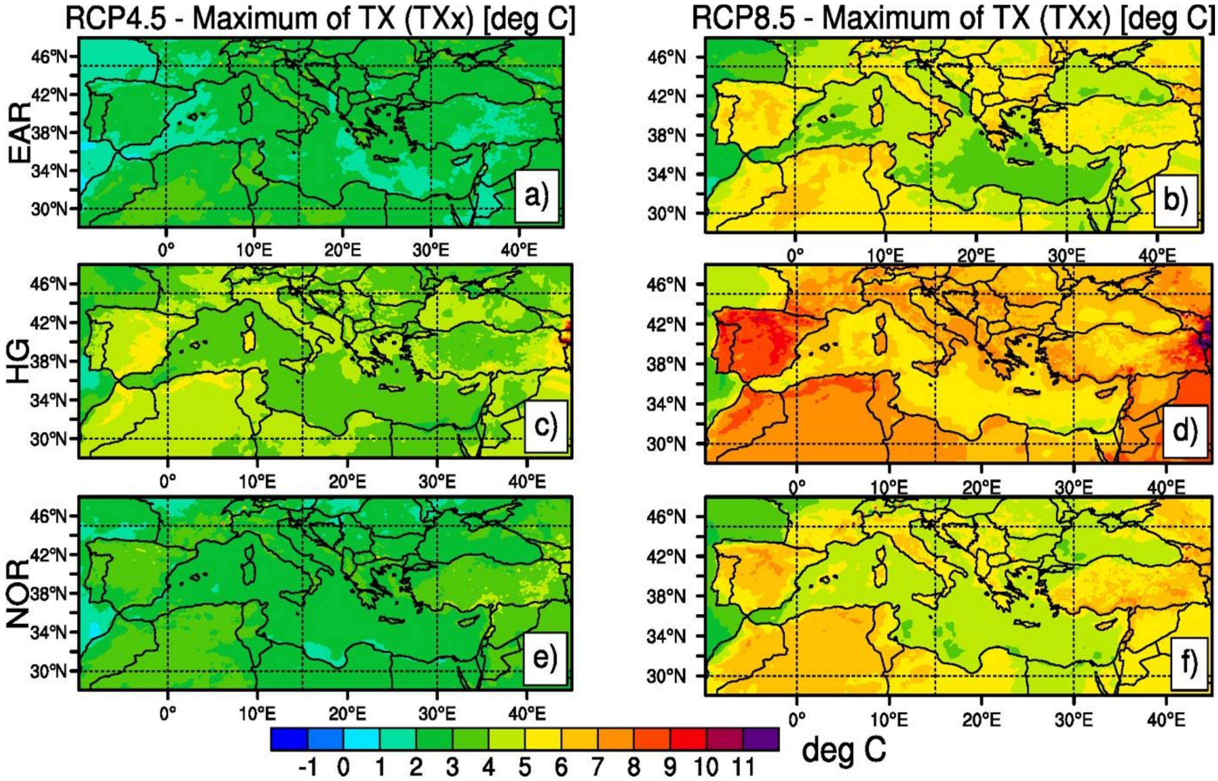

Figure 19. The temporally averaged changes in the TXx (°C) for 2071–2100 presented as differences compared to 1971–2000 under RCP4.5 (1st column), and RCP8.5 (2nd column) by using outputs of HIRHAM5 driven EC-EARTH (the first row), HadGEM2-ES (the second row) and NorESM1-M (the third row).

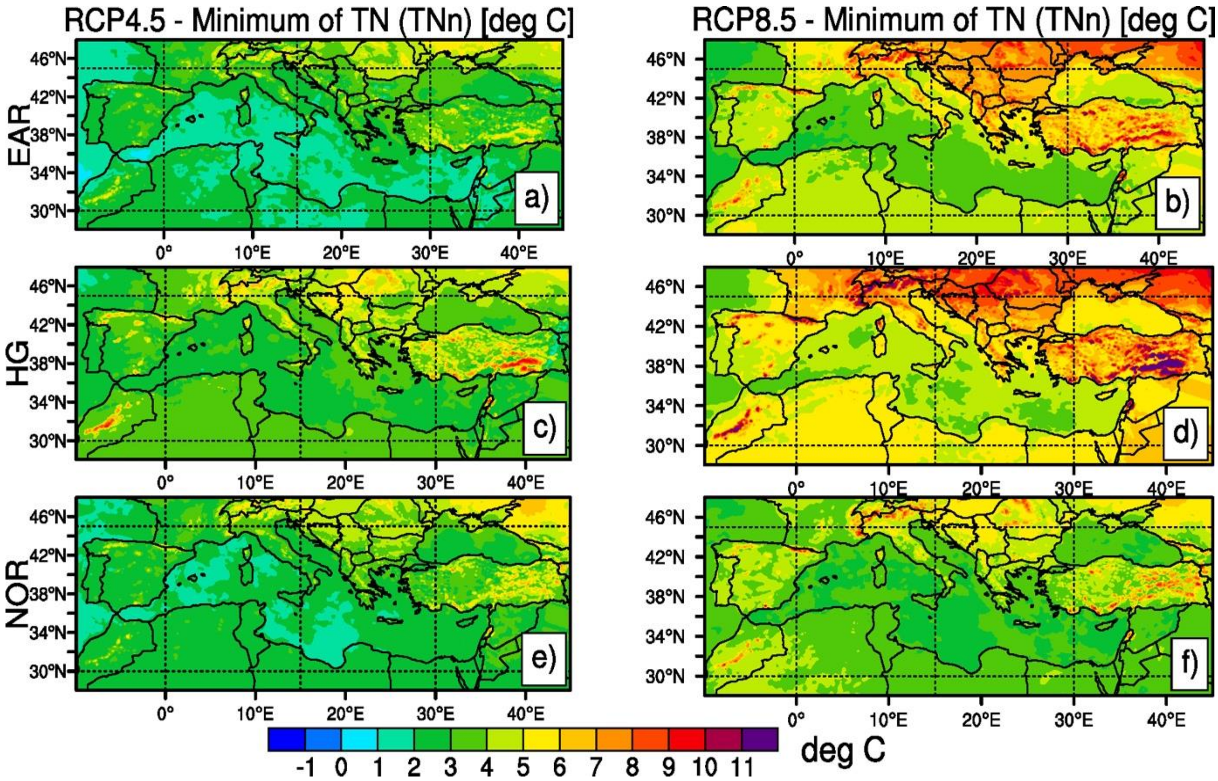

Figure 20. The temporally averaged changes in the TNn (°C) for 2071–2100 presented as differences compared to 1971–2000 under RCP4.5 (1st column), and RCP8.5 (2nd column) by using outputs of HIRHAM5 driven EC-EARTH (the first row), HadGEM2-ES (the second row) and NorESM1-M (the third row).

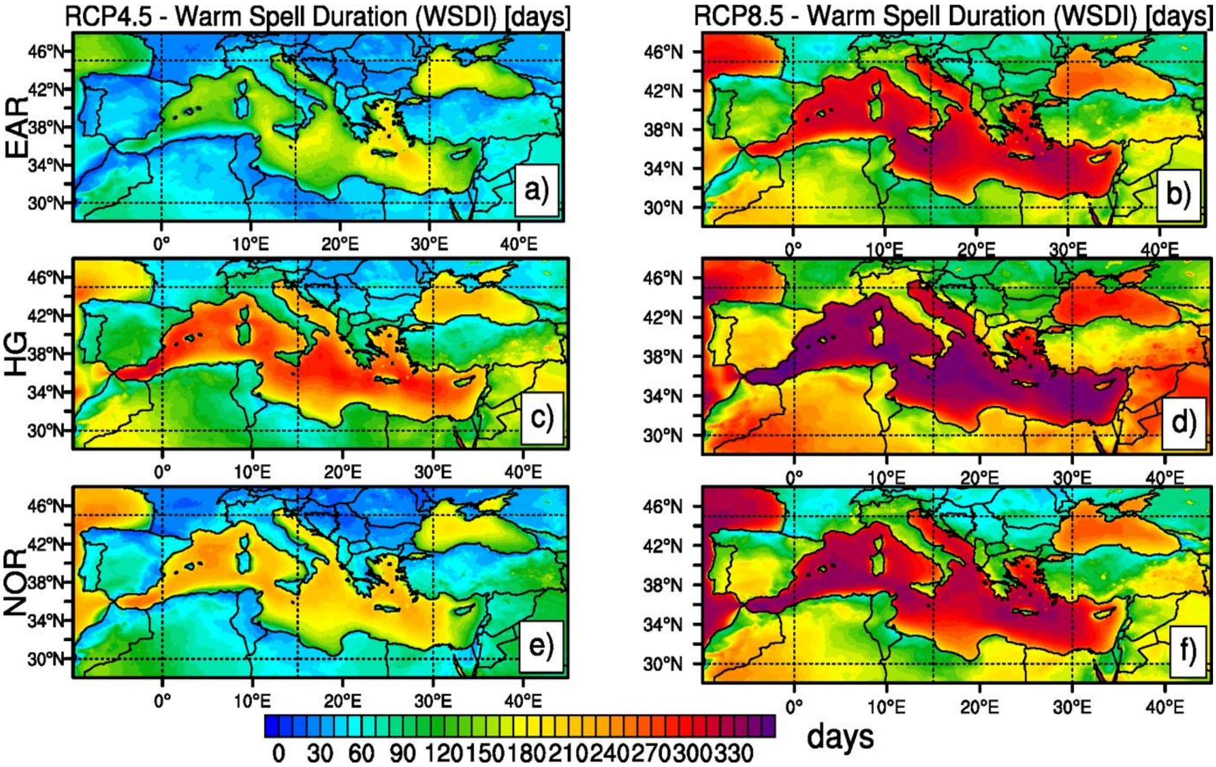

Figure 21. The temporally averaged changes in the WSDI (in days) for 2071–2100 presented as differences compared to 1971–2000 under RCP4.5 (1st column), and RCP8.5 (2nd column) by using outputs of HIRHAM5 driven EC-EARTH (the first row), HadGEM2-ES (the second row) and NorESM1-M (the third row).

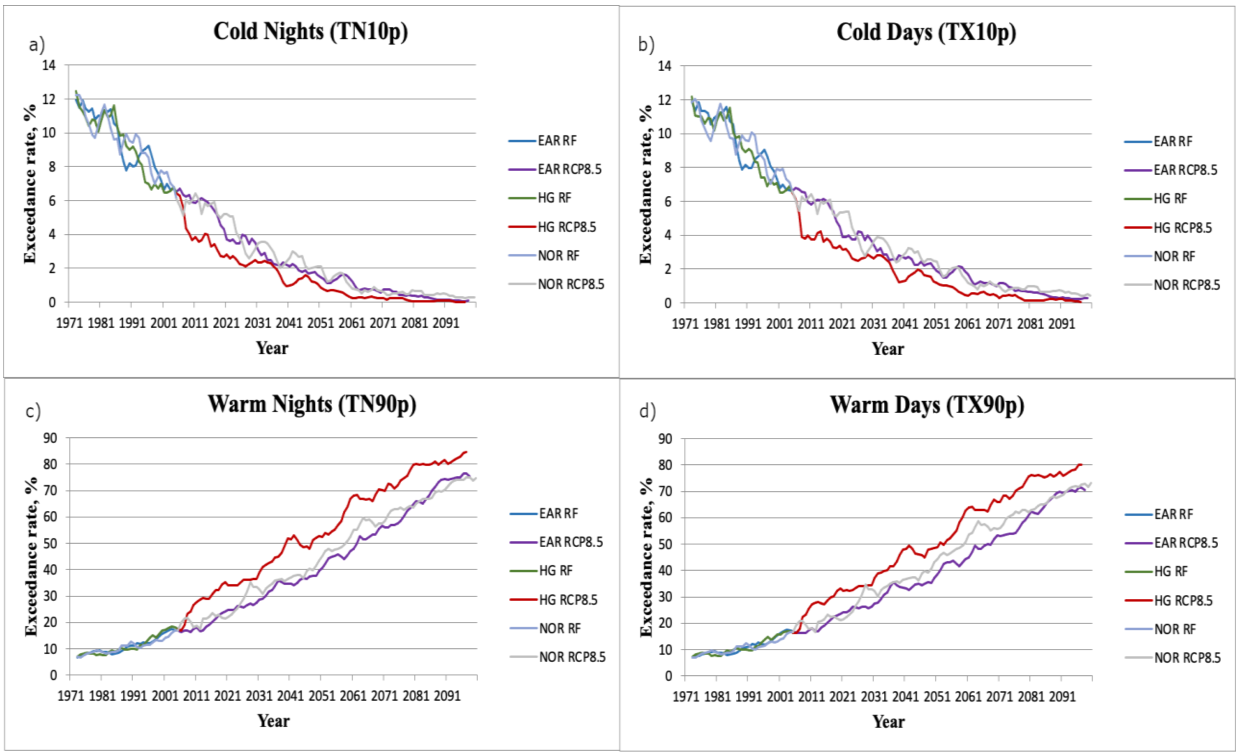

Figure 22. Spatial averages of cold nights (TN10p) (a), cold days (TX10p) (b), warm nights (TN90p) (c), and warm days (TX90p) (d) over the region as simulated by the model results for the RCP8.5. Data is smoothed by a taking 5-year running mean.

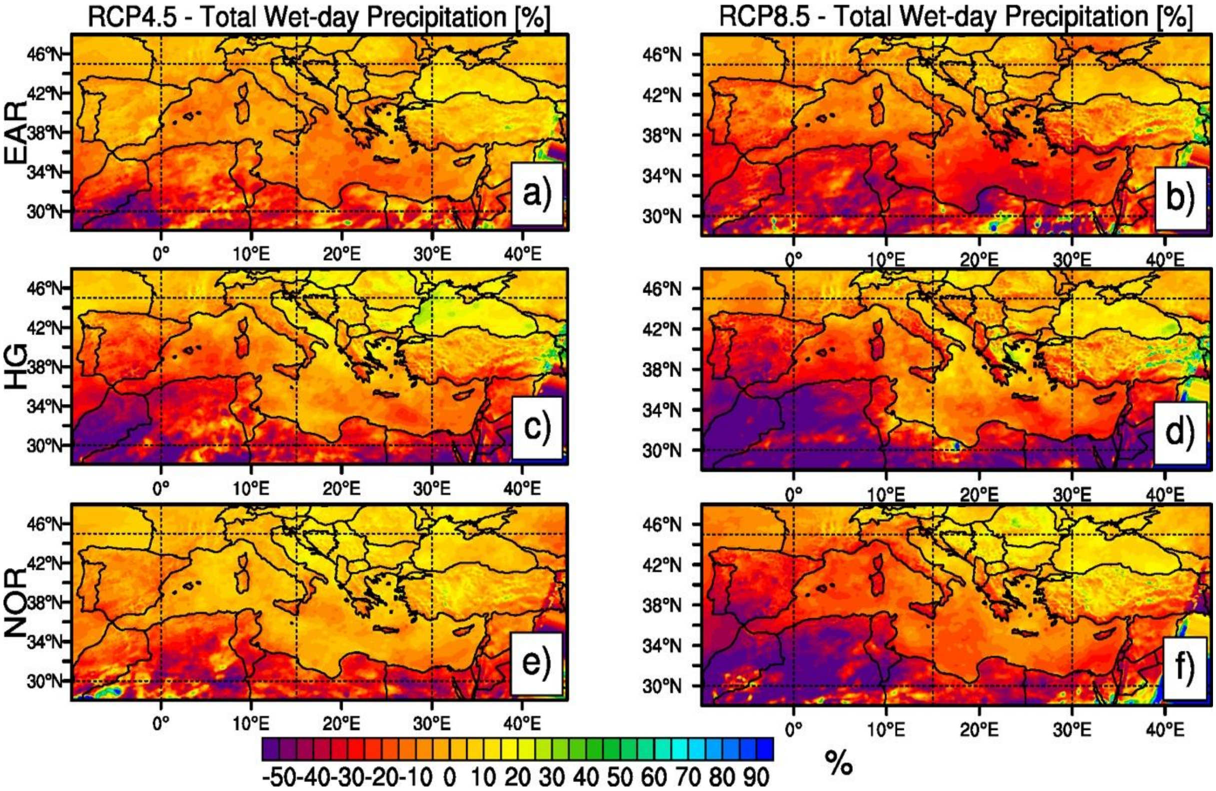

Figure 23. The temporally averaged changes in total wet-day precipitation for 2071–2100 displayed (in %) compared to 1971–2000 for RCP4.5 (1st column), and RCP8.5 (2nd column) by using outputs of HIRHAM5 driven EC-EARTH (the first row), HadGEM2-ES (the second row) and NorESM1-M (the third row).

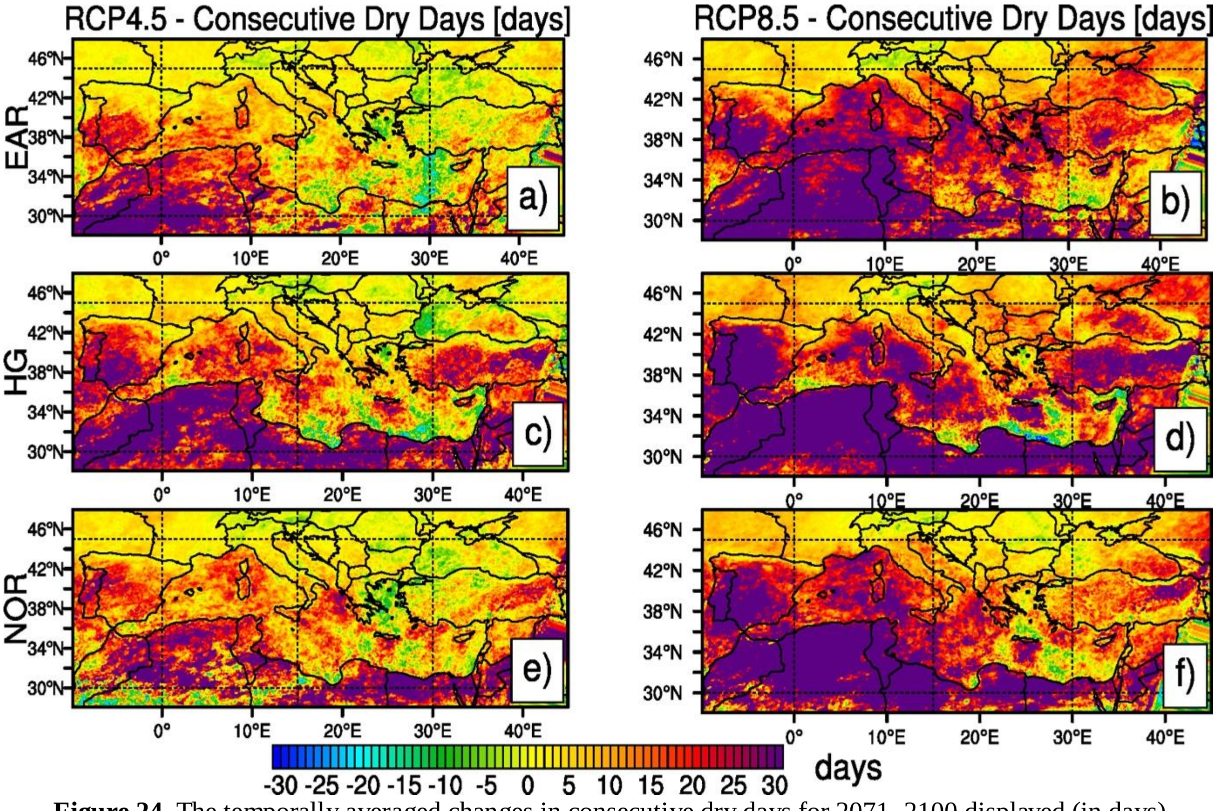

Figure 24. The temporally averaged changes in consecutive dry days for 2071–2100 displayed (in days) compared to 1971–2000 for RCP4.5 (1st column), and RCP8.5 (2nd column) by using outputs of HIRHAM5 driven EC-EARTH (the first row), HadGEM2-ES (the second row) and NorESM1-M (the third row).

IV. CONCLUSION

In this study, future change in temperature and precipitation climatology and extreme climate indices over the Mediterranean Basin including Turkey were investigated using HIRHAM5 forced by EC-EARTH, HadGEM2-ES, and NorESM1-M global climate models for three future periods of 2011– 2040, 2041–2070, and 2071–2100. First, the ability of the HIRHAM5 in reproducing the observed conditions was investigated for 1971–2000 compared to ERA-interim and CRU datasets. Performance of HIRHAM5 is reasonable except cold bias around mountainous regions and wet bias has already been observed in the RegCM result. According to results, an increase in temperatures over all parts of the domain with stronger warming for summer will be expected. Results of the HadGEM2-ES global climate model mostly show more warming than the results of EC-EARTH and NorESM1-M global model projections. This result could be very likely because of the high response of HadGEM2-ES to the doubling of CO2 concentrations in the atmosphere. It is important to see all range of changes in future climate over the region. A decrease in precipitation will likely occur in almost all parts of the region except in winter. Most of the drier weather conditions will be expected especially in winter over western and southern Turkey. This result is essential because those parts of Turkey usually get most of its precipitation in the winter. A relative decrease in the precipitation is not severe in the model outputs since the region is already arid and semi-arid in the summer months.

Projected changes in extreme climate indices defined by ETCCDI were also investigated by using outputs of HIRHAM5. Results show that an intensification of extreme weather events will be expected with increasing radiative forcing. Increase TNn are more pronounced particularly over the northern part of the Mediterranean Basin. On the other hand, increases in TXx are moderate over land areas. Stronger increases will be observed in summer over the region. The temporal evolutions of extreme climate indices show that changes will be stronger with the time and will be the strongest at the end of the century. According to the results, a decrease in total wet-day precipitation is anticipated. Longer dry spells are projected to occur as indicated by CDD results.

Model results are also in line with regional climate model RegCM driven by HadGEM2-ES which simulates an increase of between 3 °C and 7 °C in mean air temperatures of Turkey depending on the scenario. This warming will be more severe in warm seasons than in cold seasons [30]. The results obtained in this study show that Turkey and the Mediterranean region will be greatly affected by climate change due to generally increasing air temperatures and decreasing precipitation. The southern and mid-south regions of Turkey which have already low precipitation and very hot climate will be expected to have drier and warmer weather conditions. All these results also clearly reveal that Turkey's level of vulnerability to future human-induced climate change and to its possible consequences is very high.

ACKNOWLEDGEMENT

The author is grateful to Jens Hesselbjerg Christensen for valuable suggestions, comments, and support, and also to Fredrik Boberg and Ole Bøssing Christensen from Danish Meteorological Institute for data provided for this study. The author was supported by the Scientific and Technological Research Council of Turkey (TUBITAK) under the program TUBITAK 2219 - International Postdoctoral Research Fellowship.

REFERENCES

[1] IPCC, 2021: Climate Change 2021: The Physical Science Basis. Contribution of Working Group I to the Sixth Assessment Report of the Intergovernmental Panel on Climate Change [Masson-Delmotte, V., P. Zhai, A. Pirani, S.L. Connors, C. Péan, S. Berger, N. Caud, Y. Chen, L. Goldfarb, M.I. Gomis, M. Huang, K. Leitzell, E. Lonnoy, J.B.R. Matthews, T.K. Maycock, T. Waterfield, O. Yelekçi, R. Yu, and B. Zhou (eds.)]. Cambridge University Press. In Press.

[2] Giorgi, F. (2006). Climate change hot-spots. *Geophys. Res. Lett.*, *33*(8). L08707, https://doi.org/10.1029/2006GL025734.

[3] Lionello, P., Malanotte-Rizzoli, P., Boscolo, R., Alpert, P., Artale, V., Li, L., ... and Xoplaki, E. (2006). The Mediterranean climate: an overview of the main characteristics and issues. In: Lionello P, Malanotte-Rizzoli P, Boscolo R (eds) Mediterranean Climate Variability. Amsterdam, Elsevier, pp 1–26. https://doi.org/10.1016/S1571-9197(06)80003-0

[4] Lionello, P., Abrantes, F., Congedi, L., Dulac, F., Gacic, M., Gomis, D., ... and Xoplaki, E. (2012). Introduction: mediterranean climate—background information. In *The climate of the Mediterranean region: From the past to the future* (pp. xxxv-xc). Elsevier Inc. ISBN: 9780124160422. https://doi.org/10.1016/B978-0-12-416042-2.00012-4.

[5] Giorgi, F., and Lionello, P. (2008). Climate change projections for the Mediterranean region. *Glob. Planet. Chang.*, *63*(2-3), 90-104. https://doi.org/10.1016/j.gloplacha.2007.09.005

[6] Diffenbaugh, N. S., and Giorgi, F. (2012). Climate change hotspots in the CMIP5 global climate model ensemble. *Clim.*

Chang., *114*(3), 813-822. doi:10.1007/s10584-012-0570-x.

[7] Lionello, P., and Scarascia, L. (2018). The relation between climate change in the Mediterranean region and global warming. *Reg. Environ. Change*, *18*(5), 1481-1493.

[8] Christensen, J. H., Hewitson, B., Busuioc, A., Chen, A., Gao, X., Held, I., ... and Whetton, P. (2007). Regional climate projections. In: Solomon S, Qin D, Manning M, Chen Z, Marquis M, Averyt KB, Tignor M, Miller HL (eds) Climate change 2007: the physical science basis. Contribution of Working Group I to the Fourth Assessment Report of the Intergovernmental Panel on Climate Change. Cambridge University Press, Cambridge.

[9] Christensen, J. H., and Christensen, O. B. (2007). A summary of the PRUDENCE model projections of changes in European climate by the end of this century. *Clim. Change*, *81*(1), 7-30.

[10] Planton, S., Lionello, P., Artale, V., Aznar, R., Carrillo, A., Colin, J., ... and Tsimplis, M. (2012). The Climate of the Mediterranean Region in Future Climate Projections in The Climate of the Mediterranean Region. From the Past to the Future. From the Past to the Future. Elsevier (NETHERLANDS), projections, Amsterdam, pp 449–502. https:// doi.org/10.1016/B978-0-12-416042-2.00008-2.

[11] Collins, M., Knutti, R., Arblaster, J., Dufresne, J. L., Fichefet, T., Friedlingstein, P., ... and Booth, B. B. (2013). Long-term climate change: projections, commitments and irreversibility. In *Climate Change 2013-The Physical Science Basis: Contribution of Working Group I to the Fifth Assessment Report of the Intergovernmental Panel on Climate Change* (pp. 1029-1136). Cambridge University Press.

[12] Gualdi, S., Somot, S., May, W., Castellari, S., Déqué, M., Adani, M., ... and Xoplaki, E. (2013). Future climate projections. In *Regional assessment of climate change in the Mediterranean*(pp. 53-118). Springer, Dordrecht. https://doi.org/10. 1007/978-94-007-5781-3_3.

[13] Dubrovský, M., Hayes, M., Duce, P., Trnka, M., Svoboda, M., and Zara, P. (2014). Multi-GCM projections of future drought and climate variability indicators for the Mediterranean region. *Reg. Environ. Change*, *14*(5), 1907-1919. doi:10.1007/s10113-013-0562-z.

[14] Mariotti, A., Pan, Y., Zeng, N., and Alessandri, A. (2015). Long-term climate change in the Mediterranean region in the midst of decadal variability. *Climate Dyn.*, *44*(5-6), 1437-1456. doi:https://doi.org/10.1007/s00382-015-2487-3.

[15] Ozturk, T., Ceber, Z. P., Türkeş, M., and Kurnaz, M. L. (2015). Projections of climate change in the Mediterranean Basin by using downscaled global climate model outputs. *International Journal of Climatology*, *35*(14), 4276-4292.

[16] Schär, C., Vidale, P. L., Lüthi, D., Frei, C., Häberli, C., Liniger, M. A., and Appenzeller, C. (2004). The role of increasing temperature variability in European summer heatwaves. *Nature*, *427*(6972), 332-336.

[17] Sánchez, E., Gallardo, C., Gaertner, M. A., Arribas, A., and Castro, M. (2004). Future climate extreme events in the Mediterranean simulated by a regional climate model: a first approach. *Global and Planetary Change*, *44*(1-4), 163-180.

[18] Diffenbaugh, N. S., Pal, J. S., Giorgi, F., and Gao, X. (2007). Heat stress intensification in the Mediterranean climate change hotspot. *Geophysical Research Letters*, *34*(11).

[19] Goubanova, K., and Li, L. (2007). Extremes in temperature and precipitation around the Mediterranean basin in an ensemble of future climate scenario simulations. *Global and Planetary Change*, *57*(1-2), 27-42.

[20] Meehl, G. A., Stocker, T. F., Collins, W. D., Friedlingstein, P., Gaye, A. T., Gregory, J. M., ... and Zhao, Z. C. (2007). Global climate projections. In: Climate Change 2007: The Physical Science Basis. Contribution of Working Group I to the Fourth Assessment Report of the Intergovernmental Panel on Climate Change [Solomon, S., D. Qin, M. Manning, Z. Chen, M. Marquis, K.B. Averyt, M. Tignor and H.L. Miller (eds.)]. Cambridge University Press, Cambridge, United Kingdom and New York, NY, USA.

[21] Fischer, E. M., and Schär, C. (2010). Consistent geographical patterns of changes in high-impact European heatwaves. *Nature geoscience*, *3*(6), 398-403.

[22] Sillmann, J., Kharin, V. V., Zwiers, F. W., Zhang, X., and Bronaugh, D. (2013). Climate extremes indices in the CMIP5 multimodel ensemble: Part 2. Future climate projections. *Journal of Geophysical Research: Atmospheres*, *118*(6), 2473-2493.

[23] Lelieveld, J., Proestos, Y., Hadjinicolaou, P., Tanarhte, M., Tyrlis, E., and Zittis, G. (2016). Strongly increasing heat extremes in the Middle East and North Africa (MENA) in the 21st century. *Climatic Change*, *137*(1), 245-260.

[24] Zittis, G., Hadjinicolaou, P., Fnais, M., and Lelieveld, J. (2016). Projected changes in heat wave characteristics in the eastern Mediterranean and the Middle East. *Regional environmental change*, *16*(7), 1863-1876.

[25] Önol, B., and HM Semazzi, F. (2009). Regionalization of climate change simulations over the Eastern Mediterranean. *Journal of Climate*, *22*(8), 1944-1961.

[26] Türkeş, M., Kurnaz, M. L., Öztürk, T., Altınsoy, H. 2011. "Climate changes versus 'security and peace' in the Mediterranean macro climate region: are they correlated?". In: Proceedings of International Human Security Conference on Human Security: New Challenges, New Perspectives, p.625-639, CPRS Turkey, 27-28 October 2011: İstanbul.

[27] Sen, B., Topcu, S., Türkeş, M., Sen, B. and Warner, J. F. 2012. "Projecting climate change, drought conditions and crop productivity in Turkey", Climate Research 52, 175–191.

[28] Türkeş, M. 2012. "Küresel İklim Değişikliği ve Çölleşme". İçinde: Günümüz Dünya Sorunları – Disiplinlerarası Bir Yaklaşım (ed. N. Özgen), s.1-42. Eğiten Kitap: Ankara.

[29] IPCC. 2013. Climate Change 2013: The Physical Science Basis. Contribution of Working Group I to the Fifth Assessment Report of the Intergovernmental Panel on Climate Change [Stocker, T.F., Qin, D., Plattner, G. K., Tignor, M., Allen, S. K., Boschung, J., Nauels, A., Xia, Y., Bex, V., Midgley, P.M. (eds.)]. Cambridge University Press, Cambridge, United Kingdom and New York, NY, USA, 1535 pp, doi:10.1017/CBO9781107415324.

[30] Ozturk, T., Türkeş, M., Kurnaz, M.L. 2014. "Analysing Projected Changes in Future Air Temperature and Precipitation Climatology of Turkey by Using RegCM4.3.5 Climate Simulations", Aegean Geographical Journal, 20, 17-27.

[31] Türkeş, M., Sümer, U. M., Demir, I. 2002, "Re-evaluation of Trends and Changes in Mean, Maximum and Minimum Temperatures of Turkey for the Period 1929–1999", International Journal of Climatology, 22, 947–977.

[32] Xoplaki, E., Gonzalez-Rouco, J. F., Luterbacher, J., Wanner, H. 2003. "Mediterranean Summer Air Temperature Variability and Its Connection to the Large-Scale Atmospheric Circulation and SSTs". Climate Dynamics, 20, 723–739.

[33] Meehl, G. A., Tebaldi, C. 2004. "More Intense, More Frequent, and Longer Lasting Heat Waves in the 21st Century", Science, 305 (5686), 994-997.

[34] Diaz, J., Garcia-Herrera, R., Trigo, R. M., Linares, C., Valente, M. A., De Migule, J. M., Hernandez, E. 2006. "The Impact of the Summer 2003 Heat Wave in Iberia: How Should We Measure It?", International Journal of Biometeorology, 50, 159–166.

[35] Della-Marta, P. M., Haylock, M. R., Luterbacher, J., Wanner, H. 2007. "Doubled Length of Western European Summer Heat Waves Since 1880", Journal of Geophysical Research, 112, D15103.

[36] Fischer, E. M., Schar, C. 2010. "Consistent Geographical Patterns of Changes in High-Impact European Heatwaves", Nature Geoscience, 3(6), 398-403.

[37] Kuglitsch, F. G., Toreti, A., Xoplaki, E., Della-Marta, P. M., Zerefos, C. S., Türkeş, M., Luterbacher, J. 2010. "Heat Wave Changes in the Eastern Mediterranean Since 1960", Geophysical Research Letters, 37(4), L04802.

[38] Gao, X., and Giorgi, F. (2008). Increased aridity in the Mediterranean region under greenhouse gas forcing estimated from high resolution simulations with a regional climate model. *Global and Planetary Change*, *62*(3-4), 195-209.

[39] Bozkurt, D., and Sen, O. L. (2011). Precipitation in the Anatolian Peninsula: sensitivity to increased SSTs in the surrounding seas. *Climate dynamics*, *36*(3-4), 711-726.

[40] Bozkurt, D., Turuncoglu, U., Sen, O. L., Onol, B., and Dalfes, H. N. (2012). Downscaled simulations of the ECHAM5, CCSM3 and HadCM3 global models for the eastern Mediterranean–Black Sea region: evaluation of the reference period. *Climate dynamics*, *39*(1), 207-225.

[41] Önol, B. (2012). Effects of coastal topography on climate: high-resolution simulation with a regional climate model. *Climate Research*, *52*, 159-174.

[42] Ozturk, T., Altinsoy, H., Türkeş, M., and Kurnaz, M. L. (2012). Simulation of temperature and precipitation climatology for the Central Asia CORDEX domain using RegCM 4.0. *Climate Research*, *52*, 63-76.

[43] Önol, B., and Unal, Y. S. (2014). Assessment of climate change simulations over climate zones of Turkey. *Regional Environmental Change*, *14*(5), 1921-1935.

[44] Bozkurt, D., and Sen, O. L. (2013). Climate change impacts in the Euphrates–Tigris Basin based on different model and scenario simulations. *Journal of hydrology*, *480*, 149-161.

[45] Önol, B., Bozkurt, D., Turuncoglu, U. U., Sen, O. L., and Dalfes, H. N. (2014). Evaluation of the twenty-first century RCM simulations driven by multiple GCMs over the Eastern Mediterranean–Black Sea region. *Climate dynamics*, *42*(7-8), 1949-1965.

[46] Ozturk, T., Türkeş, M., and Kurnaz, M. L. (2014). Analysing projected changes in future air temperature and precipitation climatology of Turkey by using RegCM4.3.5 climate simulations. *Aegean Geographical Journal*, *20*, 17-27.

[47] Turp, M. T., Ozturk, T., Türkeş, M., and Kurnaz, M. L. (2014). Investigation of projected changes for near future air temperature and precipitation climatology of Turkey and surrounding regions by using the regional climate model RegCM4. 3.5. *Aegean Geographical Journal*, *23*(1), 1-24.

[48] Gürkan, H., Arabacı, H., Demircan, M., Eskioğlu, O., Şensoy, S., and Yazıcı, B. (2016). Temperature and precipitation projections based on GFDL-ESM2M using RCP4.5 and RCP8.5 scenarios for Turkey. *Turkish Journal of Geographical Sciences*, 14(2), 77- 88.

[49] Demircan, M., Gürkan, H., Eskioğlu, O., Arabacı, H., and Coşkun, M. (2017). Climate Change Projections for Turkey: Three Models and Two Scenarios. *Turkish Journal Of Water Science and Management*, 1(1), 22-43.

[50] Ozturk, T., Turp, M. T., Türkeş, M., and Kurnaz, M. L. (2017). Projected changes in temperature and precipitation climatology of Central Asia CORDEX Region 8 by using RegCM4. 3.5. *Atmospheric Research*, *183*, 296-307.

[51] Ozturk, T., Turp, M. T., Türkeş, M., and Kurnaz, M. L. (2018). Future projections of temperature and precipitation climatology for CORDEX-MENA domain using RegCM4. 4. *Atmospheric Research*, *206*, 87-107.

[52] Oğuz, K., and Akın, B. S. (2018). Evaluation of temperature, precipitation and dust aerosol simulations for Turkey. *International Journal of Current Research*, 10, (09), 73225-73233.

[53] Turkes, M., Turp, M. T., An, N., Ozturk, T., and Kurnaz, M. L. (2020). Impacts of climate change on precipitation climatology and variability in Turkey. In *Water resources of Turkey* (pp. 467-491). Springer, Cham.

[54] Ozturk, T., Tufan Turp, M., Türkeş, M., and Kurnaz, M. L. (2017, April). Investigation of high-resolution climate projections over Turkey and its surrounding regions using RegCM4. 4. In *EGU General Assembly Conference Abstracts* (p. 8020).

[55] Christensen, J. H., Carter, T. R., Giorgi, F. 2002. “PRUDENCE employs new methods to assess European climate change”, Eos, Transactions, American Geophysical Union, 83,147, doi: 10.1029/2002EO000094.

[56] Christensen, J. H., Christensen, O. 2007. “A summary of the PRUDENCE model projections of changes in European climate by the end of this century”, Climatic Change, 81, 7–30. doi: 10.1007/s10584-006- 9210-7.

[57] Van der Linden, P., Mitchell, J. e. 2009. “ENSEMBLES: Climate Change and Its Impacts-Summary of Research and Results from the ENSEMBLES Project”, Exeter: Met Office Hadley Centre.

[58] Christensen, J. H., Kjellström, E., Giorgi, F., Lenderink, G., Rummukainen, M. 2010. “Weight assignment in regional climate models”, Climate Research, 44, 179–194, doi: 10.3354/cr00916.

[59] Giorgi, F., Gutowski, W. J. 2015. “Regional dynamical downscaling and the CORDEX initiative”, Annual Review of Environment and Resources, 40, 467–490, doi: 10.1146/annurev-environ-102014-021217.

[60] Gutowski, J. W. J., Giorgi, F., Timbal, B., Frigon, A., Jacob, D., Kang, H., Raghavan, K., et al. 2016. “WCRP COordinated Regional Downscaling EXperiment (CORDEX): a diagnostic MIP for CMIP6”, Geoscientific Model Development, 9, 4087–4095, doi: 10.5194/gmd-9-4087-2016.

[61] Christensen, O. B., Drews, M., Christensen, J. H., Dethloff, K., Ketelsen, K., Hebestadt, I., Rinke, A. 2006. “The HIRHAM regional climate model version 5 (β)”, Tech Rep 06-17, Danish Meteorological Institute, Copenhagen.

[62] Box, J. E., and Rinke, A. (2003). Evaluation of Greenland ice sheet surface climate in the HIRHAM regional climate model using automatic weather station data. *Journal of Climate*, *16*(9), 1302-1319.

[63] Beniston, M., Stephenson, D. B., Christensen, O. B., Ferro, C. A., Frei, C., Goyette, S., ... and Woth, K. (2007). Future extreme events in European climate: an exploration of regional climate model projections. *Climatic change*, *81*(1), 71-95.

[64] May, W. (2008). Potential future changes in the characteristics of daily precipitation in Europe simulated by the HIRHAM regional climate model. *Climate Dynamics*, *30*(6), 581-603.

[65] Christensen, J. H., Boberg, F., Christensen, O. B., and Lucas-Picher, P. (2008). On the need for bias correction of regional climate change projections of temperature and precipitation. *Geophysical Research Letters*, *35*(20).

[66] Kotlarski, S., Keuler, K., Christensen, O. B., Colette, A., Déqué, M., Gobiet, A., ... and Wulfmeyer, V. (2014). Regional climate modeling on European scales: a joint standard evaluation of the EURO-CORDEX RCM ensemble. *Geoscientific Model Development*, *7*(4), 1297-1333.

[67] Giorgi, F., Bates, G. T., and Nieman, S. J. (1993). The multiyear surface climatology of a regional atmospheric model over the western United States. *Journal of Climate*, *6*(1), 75-95.

[68] Giorgi, F., Marinucci, M.R.,and Bates, G.T. (1993). Development of a second generation region- al climate model (regcm2) boundary layer and radiative transfer processes. *Mon. Weather Rev*, 121, 2794–2813.

[69] Undén, P., Rontu, L., Järvinen, H., Lynch, P., Calvo, J., Cats, G., Cuxart, J., Eerola, K., Fortelius, C., Garcia-Moya, J. A., Jones, C., Lenderlink, G., McDonald, A., McGrath, R., Navascues, B., Woetman Nielsen, N., Ødegaard, V., Rodrigues, E., Rummukainen, M., Rõõm, R., Sattler, K., Hansen Sass, B., Savijärvi, H., Wichers Schreur, B., Sigg, R., The, H., and Tijm, A. (2002). HIRLAM-5 Scientific Documentation. Scientific Report. http://hirlam.org.

[70] Roeckner, E., Bäuml, G., Bonaventura, L., Brokopf, R., Esch, M., Giorgetta, M., Hagemann, S., Kirchner, I., Kornblueh, L., Manzini, E., Rhodin, A., Schlese, U., Schulzweida, U., and Tompkins, A. (2003). The atmospheric general circulation model ECHAM5. Part 1. Model description. Report no. 349, Max-Planck-Institut für Meteorologie (MPI-M).

[71] Simmons, A. S., Uppala, D. D., and Kobayashi, S. (2007). ERA-Interim: new ECMWF reanalysis products from 1989 onwards, *ECMWF Newsl*., 110, 29−35.

[72] Mitchell, T.D. and Jones, P.D. (2005). An improved method of constructing a database of monthly climate observations and associated high-resolution grids. *Int J Climatol*, 25(6),693–712.

[73] Collins, W.J., Bellouin, N., Doutriaux-Boucher, M., Gedney, N., Hinton, T., Jones, C.D., Liddicoat, S., Martin, G., O'Connor, F., Rae, J., Senior, C., Totterdell, I., Woodward, S., Reichler, T., and Kim, J. (2008). Evaluation of the HadGEM2 model. Met Office Hadley Centre Technical Note No. HCTN 74.

[74] Bentsen, M., Bethke, I., Debernard, J. B., Iversen, T., Kirkevåg, A., Seland, Ø., Drange, H., Roelandt, C., Seierstad, I. A., Hoose, C., and Kristjánsson, J. E. (2013). The Norwegian Earth System Model, NorESM1-M – Part 1: Description and basic evaluation of the physical climate, *Geosci. Model Dev*., 6, 687–720, https://doi.org/10.5194/gmd-6-687-2013, 2013.

[75] Van Vuuren, D. P., Edmonds, J., Kainuma, M., Riahi, K., Thomson, A., Hibbard, K., ... and Rose, S. K. (2011). The representative concentration pathways: an overview. *Climatic change*, *109*(1), 5-31.

[76] Alexander, L. V., Zhang, X., Peterson, T. C., Caesar, J., Gleason, B., Klein Tank, A. M. G., ... and Vazquez‐Aguirre, J. L. (2006). Global observed changes in daily climate extremes of temperature and precipitation. *Journal of Geophysical Research: Atmospheres*, *111*(D5).

[77] Klein Tank, A. M. G., F. W. Zwiers, and X. Zhang (2009). Guidelines on analysis of extremes in a changing climate in support of informed decisions for adaptation, Climate data and monitoring WCDMP-No. 72, WMO-TD No. 1500, 56pp.

[78] Zhang, X., Alexander, L., Hegerl, G. C., Jones, P., Tank, A. K., Peterson, T. C., ... and Zwiers, F. W. (2011). Indices for monitoring changes in extremes based on daily temperature and precipitation data. *Wiley Interdisciplinary Reviews: Climate Change*, *2*(6), 851-870.